

Structure of the Precambrian Sedimentary Cover and Upper Part of the Basement in the Central Russian Aulacogen and Orsha Depression (East European Platform)

N. P. Chamov, V. V. Kostyleva, and A. F. Veis[†]

Geological Institute, Russian Academy of Sciences (GIN RAN), Pyzhevskii per. 7, Moscow, 119017 Russia

e-mail: nchamov@yandex.ru

Received May 25, 2009

Abstract—The Precambrian sedimentary section and upper part of the basement of the Central Russian Aulacogen and Orsha Depression, two largest structures located beneath the Moscow Syncline are analyzed. It has been established that the Late Riphean Central Russian Aulacogen was initiated on the Proterozoic crust of the Transcratonic belt that separates different-aged geological blocks of the East European Platform basement. The Orsha Depression is superposed both on sedimentary complexes of the aulacogen and rocks constituting structures surrounding the Transcratonic belt. Boundaries of the sedimentary cover and basement are outlined and a new structure (Toropets–Ostashkov Trough) is defined. The Precambrian section recovered by Borehole North Molokovo is proposed to serve as a reference one for the Central Russian Aulacogen. The CMP records demonstrate seismocomplexes, which allow one to trace rock members and sequences defined by drilling. Eight seismocomplexes, combination of which varies in different structures, are defined in the Upper Riphean–Vendian part of the sedimentary section. The section of the Central Russian Aulacogen includes the following sedimentary complexes: dominant gray-colored arkoses (R_3^1), variegated arkoses (R_3^2), red-colored arkoses (R_3^3), and volcanosedimentary rocks (V_1^1). The section of the Orsha Depression consists of dominant red-colored quartz sandstones (R_3^4), glacial and interglacial (V_1^1), and variegated volcanogenic–terrigenous sediments. The upper seismocomplex (V_2) is composed of terrigenous and terrigenous–carbonate rocks. It represents the basal unit of the Moscow Syncline, which marks the plate stage in development of the East European Platform. The upper part of the basement corresponds to a seismocomplex (Pr_1) represented by dynamometamorphosed rocks that form a tectonic mélange. Analysis of the lateral and vertical distribution of the defined seismocomplexes made it possible to specify the structure of the Riphean–Vendian part of the sedimentary cover and to revise their formation history in some cases.

DOI: 10.1134/S0024490210010049

INTRODUCTION

Mapping of the sedimentary cover is of great practical significance, since this method makes it possible to determine its composition and estimate its potential of hydrocarbon reserves, structure of reservoirs, and prospecting for many mineral resources, including placer deposits, building materials, brines, and mineral and drinking water.

Most difficulties are related to the study of sedimentary complexes accumulated in structures that were formed at the Late Precambrian tectonic stage of the East European Platform development. The main structures among them are the Central Russian Aulacogen and Orsha Depression located at the Moscow Syncline basement. Despite long-term studies of these structures, many basic aspects of their tectonic

development, lithology, and stratigraphy of sedimentary sequences therein remain unclear so far.

Geodynamic nature of the Central Russia Aulacogen and Orsha Depression remains debatable so far. Moreover, exact boundaries and internal structure of the aulacogen, the number of troughs therein included, are still unknown because of its complex structure, although these features are of primary significance for establishing the volume of the sedimentary cover and estimating its mineragenic potential.

These issues remain crucial since studies by N.S. Shatsky, who proposed the notion of *aulacogen* as a new type of structures within ancient platforms. In particular, as early as the 1960s, Shatsky assumed the development of a graben-shaped trough in the axial part of the Moscow Syncline (Shatsky, 1964). Precisely this trough was subsequently termed as the Central Russian Aulacogen. Further studies revealed that the aulacogen represents a composite structure con-

[†] Deceased.

sisting of numerous smaller troughs, which are displaced along faults relative to each other.

Similar to the Orsha Depression, flank elements of the Central Russian Aulacogen (Valdai–Kresttsy and Kotlas–Yaren troughs) were defined in the basement relief by E.E. Fotiadi in the terminal 1950s based on the interpretation of gravimetric survey and rare drilling data. Based on interpretation of data obtained by the complex refraction logging method, P.S. Khokhlov first proposed the notion that the Moscow Syncline basement includes a complex tectonic structure represented by a system of troughs (rather than a single trough) separated by swell-shaped basement uplifts. The concept of the Central Russian Aulacogen as a system of two parallel “furrows” separated by a horst was shared by many geologists (Nagornyi, 1990; Ostrovskii, 1974; Ostrovskii et al., 1975; Valeev, 1978; Valeev et al., 1969). The “furrows” were divided into troughs of the “northern” (Kresttsy, Molokovo, Kes’ma, and others) and “southern” (Moscow region troughs, such as the Gzhatsk, Moscow region, and other depressions included) branches.

In 1993, based on seismic data, Yu.B. Konoval’tsev from Expedition no. 2 of the Spetsgeofizika Federal State Unitary Enterprise defined the Tver Trough, a large negative structure extending parallel to the Valdai, Molokovo, and Kes’ma troughs.

The Hypsometric Map of the Basement Surface (Kapustin et al., 2001) represents an important generalization of these studies. According to the map, the Central Russian Aulacogen represents a “bident fork” structure formed by two troughs converging toward the Yaren Depression. It was established that the Tver Trough forms an external southern branch of the aulacogen and Moscow region grabens are structurally isolated from the Central Russian Aulacogen.

The Volyn–Orsha paleotrough is likely the southwestern continuation of the Central Russia Aulacogen. At present, the Volyn–Central Russian system is considered a single Riphean lineament (Aizberg et al., 1986; Garetsky, 1995, 1999; Nagornyi, 1990; Razlomy..., 2007).

Issues of the genesis of sedimentary complexes remain still debatable. This statement is valid both for the reconstruction of paleosedimentation settings and for the determination of sources of detrital material. In addition, many researchers assume a wide distribution of volcanogenic and volcanosedimentary rocks in the aulacogen (Gordasnikov and Troitskii, 1966; Nikolaev, 1999; Kheraskova et al., 2001, 2002).

With the accumulation of new data, views on stratigraphy of Riphean sediments in troughs of the Central Russia Aulacogen underwent repeated revisions and refinements. Many researchers (Aksenov, 1998; Geisler, 1966; Keller, 1968; Kirsanov, 1968; Klevtsova, 1976, 2000, 2003; Kuz’menko and Shik, 2006; and others) contributed much to understanding of the Precambrian cover structure. Much attention

was paid to correlation between Riphean sections of the aulacogen and Orsha Depression.

Recent views on stratigraphic relationships between Riphean sediments are reflected in the refined working scheme of the Interdepartmental Stratigraphic Commission (Kuz’menko and Shik, 2006). According to this scheme, the *Kresttsy Group* of the Valdai Trough, for example, is correlated with Middle Riphean sediments of the Orsha Depression and Middle Riphean *Bologoe and Putilovo groups* developed in the Bologoe and Molokovo troughs of the Central Russia Aulacogen. The *Dvoretz Formation* corresponds to the *Molokovo Formation* in the Bologoe and Molokovo troughs of the Central Russia Aulacogen and the *Orsha Formation* in the Orsha Depression.

Riphean sections of the Orsha Depression were subdivided into various stratigraphic units in different years. Until the mid-1970s, pre-Lower Vendian sediments were attributed to the Upper Riphean (Veretennikov et al., 2005). Subsequently, the *Sherovichi Group* (R_1), *Belarus Group* (R_2), and *Lapich Formation* (R_3) were defined among these sediments (Makhnach et al., 1973 among others). At present, the *Sherovichi Group* and *Belarus Group* of the Orsha Depression are referred to the Middle Riphean, whereas the *Lapich Formation* is attributed to the Late Riphean. Modern concepts of stratigraphy of the Volyn–Orsha system of troughs are reflected in the Riphean correlation scheme of Belarus (Veretennikov et al., 2005).

The above-mentioned correlation schemes represent significant generalizations and play an important role in understanding the structure of the study region. Most researchers admit the confinement of preplate sediments to structurally autonomous sedimentary basins (grabens). The sediments filling individual grabens are considered stratigraphic subzones, which differ in completeness of the section and local stratigraphic units therein (Kuz’menko and Shik, 2006). The Lower Riphean sediments are missing in the entire Central Russian Aulacogen and Orsha Depression.

At the same time, issue of correlation between Precambrian sedimentary complexes is far from its solution. This is explained primarily by the irregular study of preplate sediments, insufficient quantity of deep boreholes with good recovery, outdated information about the isotopic age of rocks, and lack of methods for dating the red-colored arkosic and quartzose sediments.

It should be emphasized that stratotypes of numerous local stratigraphic units (groups, formations, and subformations), are represented by sections of some boreholes. Lack of correlation in seismic records hampers the correlation of such units and the tracking of real geological bodies (sequences, members, and beds) along the aulacogen strike. In addition, when defining stratotypes, the researchers ignored the borehole position both in the structure of an individual trough and

in the whole ensemble of the Central Russian Aulacogen.

The seismocomplexes defined above can be used as correlative elements of the section for the solution of all these issues. Such an approach is aimed at the mapping of real geological bodies with the determination and tracking of seismic complexes in the wave pattern of CMP records. Such complexes correspond to different lithological units (members or sequences) that are readily recognized based on their facies features and mineral–petrographic properties, which are well known from drilling data (primarily, the North Molokovo parametric borehole drilled in the central part of the Central Russian Aulacogen but ignored in the existing stratigraphic schemes).

The article is dedicated to discussion of materials obtained during the long-term study of the upper part of the consolidated crust and preplate sedimentary section of the Central Russian Aulacogen and Orsha Depression. This work was accomplished in close cooperation with specialists from the Federal state unitary enterprises (FGUP), such as Nedra (Yaroslavl), Spetsgeofizika (Emmaus Settlement), IGRiGI (Moscow), and VNIIGeofizika (Moscow), as well as the Rifei group (Moscow), Geological Department of the Ministry of Natural Resources and Environment Protection of Belarus Republic (Minsk), and Institute of Geology and Geophysics of the National Academy of Sciences of Belarus (Minsk).

The main scientific tasks were as follows: (1) refinement of the spatial position of structural elements of the Central Russian Aulacogen; (2) investigation of the lithological and facies compositions of sedimentary complexes in the central part of the Central Russian Aulacogen; and (3) correlation of sedimentary complexes of the Central Russian Aulacogen and Orsha Depression.

METHODS

The choice of methods was dictated by the complex pattern of the main study objects (sedimentary basins). We followed principles of the multidisciplinary analysis discussed in (*Osadochnye...*, 2004). We used the following materials and data: magnetic fields; seismic records obtained along CMP profiles; drill cores; petrographic thin sections, including collections kindly placed at our disposal by N.V. Veretennikov (Institute of Geology and Geophysics, National Academy of Sciences of Belarus, Minsk) and V.I. Gorbachev (Nedra Federal State Unitary Enterprise, Yaroslavl); paleontological collections; mineralogical composi-

tion of rocks; isotopic investigations; and X-ray diffraction data on the composition of the clay fraction from sedimentary rocks.

The facies and mineralogical–petrographic study of rocks was performed in the Laboratory of Comparative Analysis of Sedimentary Basins (GIN RAN). The coarse fraction (0.05–0.01 mm) of sand was extracted by sieving with the subsequent washing. The heavy and light fractions were separated in bromoform (density 2.9 g/cm³). The classification of sandy rocks by Shutov (1975) was used in this work.

Volumetric fossil forms and microphytological remains were studied by A.F. Veis in the Laboratory of Precambrian Stratigraphy (GIN RAN). Clay minerals (grain size less than 0.001 mm) were determined with a DRON-1.5 X-ray diffractometer in the Laboratory of Physical Research Methods for the Study of Rock-Forming Minerals (GIN RAN). Each preparation was studied in the air-dry, ethylene glycol-saturated, and heated (up to 550°C) states (A.L. Sokolova, analyst).

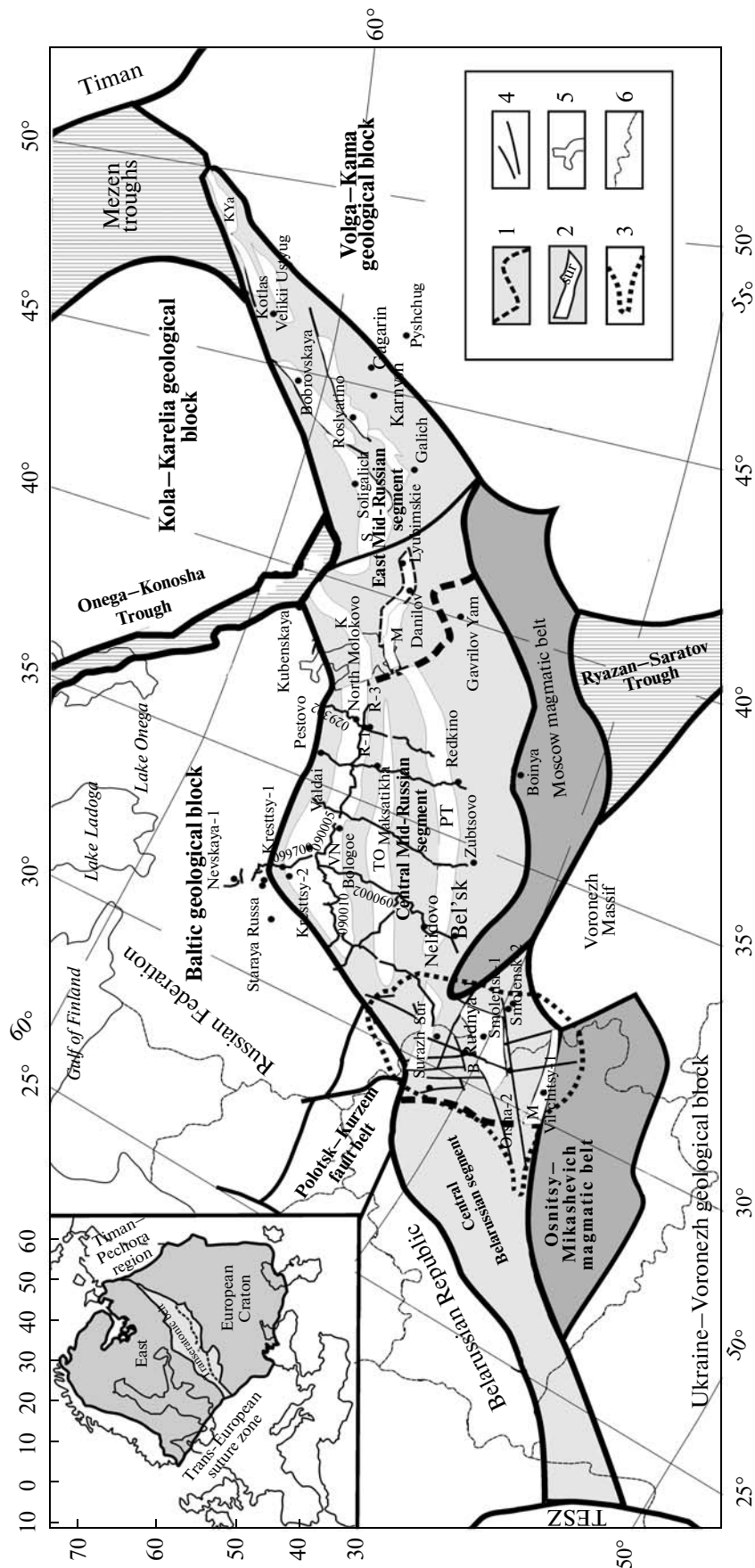
The U–Pb geochronological study of zircon and sphene fractions was conducted at the Vernadsky Institute of Geochemistry and Analytical Chemistry (Russian Academy of Sciences, Moscow). Chemical decomposition of minerals and extraction of U and Pb were performed in line with the modified technique reported in (Krogh, 1973). Concentrations of U and Pb were determined by the method of isotopic dilution with application of the mixed (²⁰⁸Pb + ²³⁵U) tracer. Corrections for the common Pb were introduced according to model values (Stacey and Kramers, 1975). The experimental data were processed using the PbDAT (Ludwig, 1991) and ISOPLOT (Ludwig, 1999) software packages.

GEOLOGICAL POSITION OF THE CENTRAL RUSSIAN AULACOGEN AND ORSHA DEPRESSION

The Central Russian Aulacogen is confined to the Proterozoic crust of the Transcratonic belt that separates different-aged geological blocks of the East European Platform basement.

The Transcratonic belt of the Proterozoic crust is the longest element of the East European Platform basement (Fig. 1). The belt traced from the Timan–Pechora region in northeast to the Trans-European suture zone in southwest is located in territories of Russia, Belarus, and Ukraine. This is a region characterized by linear patterns of the Proterozoic crust, which consolidated in the period of 1.6–1.8 Ga (Bogdanova, 1993; Garetsky, 1999; Bogdanova et al.,

Fig. 1. Schematic location of troughs in the Central Russian Aulacogen and Orsha Depression and seismic profiles of boreholes. (1) Transcratonic belt and boundaries of segments; (2) troughs of the Central Russian Aulacogen initiated on the crust of the Transcratonic belt: (M) Mogilev, (V) Vitebsk, (Sur) Surazh, (VM) Valdai–Molokovo, (TO) Toropets–Ostashkov, (PT) Prechistenka–Tver, (K) Kes'ma, (D) Danilov, (S) Soligalich, (R) Roslyatino, (KYa) Kotlas–Yaren, (VU) Velikii Ustyug; (3) contour of the Orsha Depression; (4) faults; (5) shorelines; (6) state boundaries.



2001; Chamov, 2005; Gee and Stephenson, 2006). The transplatform zone is interpreted as an extension region of the consolidated crust that experienced the influence of collisional (Kostyuchenko and Solodilov, 1997; Aksenov, 1998) or accretionary (Vladimirov et al., 2001) processes.

Seismic models of the consolidated crust structure reflect significant variations of its properties in different segments of the Transcratonic belt. Along the belt strike, the Moho surface gradually rises from a depth of approximately 50 km in southwest to 40–42 km in northeast. Its uplift is generally discordant relative to the Transcratonic belt strike: the maximal thinning zone of the crust crosses the Transcratonic belt and extends in the submeridional direction from the Onega and Mezen structures to the Kursk zone of the Voronezh Massif (Nagornyi, 1990; Kostyuchenko et al., 1995, 1996; Kostyuchenko and Solodilov, 1997; Kostyuchenko and Ismail-Zade, 1998; Garetsky et al., 1999; *Razlomy...*, 2007). Three large segments are defined in the belt: Central Belarusian, Central Mid-Russian, and East Mid-Russian (Fig. 1).

Differences in the crust structure were likely responsible for different intensities of its extension during the Late Riphean. The East Mid-Russian segment comprises two branches of deep narrow shear basins (Kapustin et al., 2001; Vladimirova et al., 2001). The en echelon pull-apart basins are largely filled with gray-colored sediments of deep lakes (Chamov et al., 2003).

In the Central Mid-Russian segment, the Upper Riphean extension was more intense and produced a system of near-parallel pull-apart basins.

The northernmost Valdai–Molokovo Trough is scrutinized by drilling and seismic works. Recent seismic studies carried out by the VNII Geofizika Federal State Unitary Enterprise along the Valdai–Demyansk–Nakhod–Toropets–Velizh–state boundary transect, reinterpretation of seismic materials obtained along the Cherikov–Orsha–Usvyaty profile in the Orsha Depression (*Razlomy...*, 2007), and our analysis of seismic records obtained by the Spetsgeofizika Federal State Unitary Enterprise allowed us to substantially refine the structure and boundaries of the Central Russian Aulacogen.

For example, the analysis of seismic records along profiles 02301 and EV-1 oriented across the Central Mid-Russian segment confirmed the presence of the southern branch of the aulacogen (Tver Trough). The western continuation of this trough is represented by a negative structure near the Bel'sk basement uplift. In this work, we consider both structures as the single Prechistenka–Tver Trough that forms the southern branch of the Central Russian Aulacogen (Fig. 1).

Discovery of the central structural branch of the aulacogen, a new large negative structure, which we termed as "Toropets–Ostashkov Trough" (Fig. 1), represents a principally new result derived from the

analysis of seismogeological data. The trough is readily recognized along several seismic profiles (09002, 007, 008, Toropets–Velizh). It is separated from neighboring troughs by basement uplifts. Seismic complexes filling this trough defined in the wave patterns of CMP records are reliably correlated with their counterparts in the neighboring troughs.

In general, sedimentary basins corresponding to each of the three troughs of the Central Mid-Russian segment are shallower and wider as compared with basins of the East Mid-Russian segment. They are filled with sediments of a wider facies spectrum of sediments ranging from the gray-colored sediments of deep lakes to the red minerals of intermontane depressions (Chamov et al., 2003). Such a distinct facies transition from "flysch" to "molasse" combined with expansion of sedimentation area points to two extension stages with different intensities (Chamov, 2005).

At present, most researchers place the southwestern boundary of the Central Russian Aulacogen along the Toropets–Velizh dislocation zone, i.e., near the Russian Federation/Belarus Republic state boundary. Previously, based on the aulacogen structure, we assumed its continuation in the Belarus territory (Chamov et al., 2003; Chamov, 2005). New geological–geophysical materials obtained during the study of transboundary structures allow us to substantiate this assumption based on actual facts.

For example, transboundary structures (known as the Vitebsk and Mogilev troughs separated by the Central Orsha horst), which are recovered by drilling (boreholes Vil'chitsy-1 and Rudnya-1) and crosscut by the Cherikov–Orsha–Usvyaty seismic profile, and the recently established graben-shaped trough located north of the Surazh basement uplift (*Razlomy...*, 2007) should be attributed to the Central Russian Aulacogen. These relicts of sedimentary basins (basin?) are filled with red-colored arkosic sediments and overlain with an erosional surface by the highly mature quartzose sandstones of the Orsha Depression. The latter depression represents a superimposed synclinal structure that was formed above the southwestern flank of the Central Russian Aulacogen. The depression extends in the submeridional direction over approximately 300 km (width 120–250 km). The structure of the Orsha Depression is scrutinized in the monograph by Belarusian geologists (*Razlomy...*, 2007). Thus, the Central Russian Aulacogen terminates in west at approximately 30° E beneath sediments of the Orsha Depression.

The Moscow region and Osnitsy–Mikashovich magmatic belts represent a specific feature of the Transcratonic belt. Similar ages of the crust (1.9–2.0 Ga), similar composition of highly magnetic rocks therein, and wide manifestation of dynamometamorphism allow us to consider them as a single lithotectonic complex. The available data on the Shchelkovo horst (Bogdanova et al., 2004) and Bel'sk basement uplift (Chamov and Gorbachev, 2004) areas provide suggest

that this belt was tectonically exhumed from deep levels of the Transcratonic belt.

The autonomous asymmetric Pavlov Posad, Moscow region, and Gzhatsk half-grabens located in the Moscow belt represent fault-line depressions that are distinctly differ (in the sedimentary section structure) from basins of the Central Russian Aulacogen (Simanovich, 2000; Kostyleva et al., 2001).

THE STRUCTURE OF THE REFERENCE SECTION OF THE CENTRAL RUSSIAN AULACOGEN

The North Molokovo parametric borehole is the latest one among boreholes drilled in the Central Russian Aulacogen. It is characterized by good recovery and was studied in detail during joint works of industrial and scientific organizations, the Nedra Federal State Unitary Enterprise and the Geological Institute of the Russian Academy of Sciences included. In addition, it is located in the central part of the Central Russian Aulacogen and may serve as a reference section for stratigraphic units defined in different boreholes. Below, we provide the characteristics of the upper part of the basement and the Precambrian sedimentary section.

Tectonic Mélange Series (Lower Proterozoic, Upper Karelian Erathem)

The tectonic mélange series comprises metamorphic rocks of the Molokovo basin basement recovered by drilling in the depth interval of 3185–3313 m.

Based on geophysical methods, thickness of the tectonic mélange sequence is estimated at 350 m. Its rocks characterize the upper geophysically “anomalous” part of the crust with low (4.9–5.1 km/s) velocities of seismic waves and stratified patterns of the wave field (Fig. 2).

The study of recovered rocks revealed their structural and lithological heterogeneities. The series is largely composed of blastomylonites developed after migmatites. The geochemical identity of these rocks indicates an isochemical character of blastomylonitization. Spessartite dikes are also present.

The rocks demonstrate distinct features of dislocation metamorphism, undoubtedly indicating their formation under the influence of large-scale tectonic processes.

The U–Pb isotopic ages obtained for zircon and sphene show that rocks of the basement were formed in the period of 2500 to 1750 Ma, i.e., they correspond to the Lower Proterozoic (Fig. 2, table).

The series consists of the mylonitic and blastomylonitic sequences.

The *mylonitic sequence* is presumably developed in the depth interval of 3210–3185 m.

No core was obtained for this interval. According to A.N. Ugryumov and A.M. Provorov (KamNIIGIS, Perm), slime fragments recovered from the depth of 3199 m contain gneissose rocks consisting of plagioclase, microcline, orthoclase, quartz, and amphibole. Plagioclases are partly replaced by the clayey hydromicaceous material.

The complex interpretation of GIS materials performed in the Tver’geofizika Scientific–Industrial Center in 1999 shows that the member is represented by compact low-porosity rocks. According to gamma–gamma density logging data, rock density amounts to 3.0–3.1 g/cm³. Porosity in some intervals is negligible (fractions of the percent) and usually does not exceed 6–12%. Specific electric resistance in this interval increases up to 100n–1000n Ohm/m. Therefore, possibilities of the side logging and side micrologging methods are limited.

The profilometry data indicate high hardness and confining properties of rock and absence of fracturing. Caverns and furrows are missing in this interval, but they complicate significantly the borehole below 3210 m.

These data and positions of rocks in the section suggest their formation as the result of mylonitization, i.e., transformation due to crushing and grinding of rocks along tectonic fracture zones in the course of dislocation metamorphism. The mylonites represent finely grinded (partly recrystallized and cemented) rocks. Mylonitization is most intense in the quartz-enriched rocks (granites, gneisses, and others), since quartz is a mineral most sensitive to pressure-induced destruction (Sklyarov et al., 1997).

It is most probable that the mylonite formation was related to the exhumation of remaining rocks according to the exhumation mechanism of metamorphic core complexes. This concept is substantiated elsewhere (Chamov et al., 2002, 2003; Chamov, 2005). If this assumption is correct, rocks of this member are characterized by the youngest (Late Riphean) age, which corresponds to initiation of the Molokovo basin structure. Rocks of precisely this member could become an important source of clastic material for basal units of the Molokovo basin.

The *blastomylonitic sequence* is recovered in the depth interval of 3210 to 3313 m.

Intense deformation and disintegration of rocks, on the one hand, and processes of recrystallization and neoformation, on the other hand, suggest that this sequence can be considered tectonoblastic metamorphic rocks (blastomylonites). With regard to structure, the sequence represents a tectonic mélange, in which the blastomylonitic matrix encloses relicts of the primary migmatized granitoid rocks and amphibolites. The transformation degree of all rocks from this sequence corresponds to the epidote–amphibolite metamorphism facies. No increase in the metamorphism degree with depth is observed.

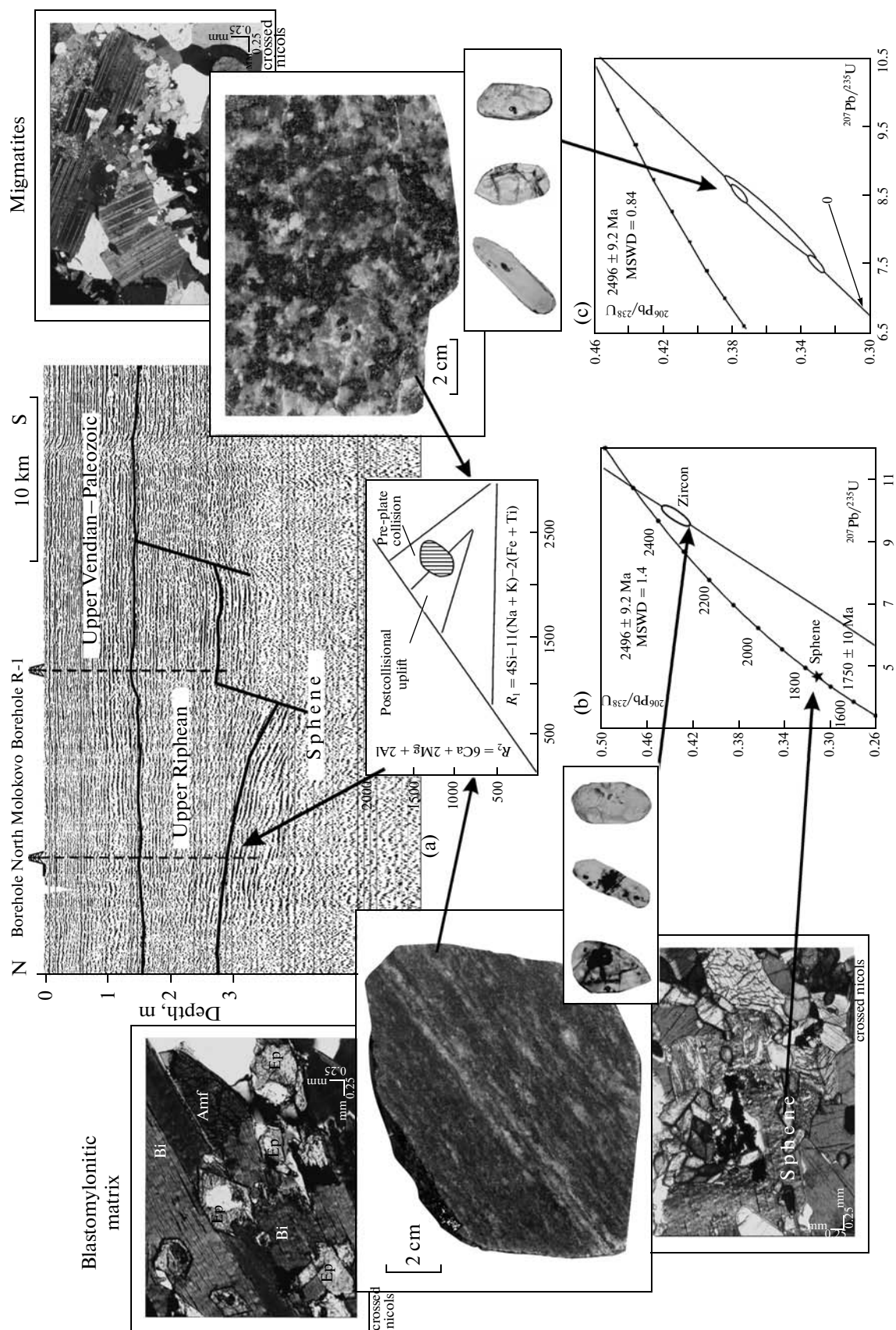


Fig. 2. Fragment of time section along profile EV-1 with photographs of type samples from the upper part of the basement recovered by Borehole North Molokovo. (a) Geodynamic affinity of rocks from tectonic melange, after (Batchelor and Bowden, 1985); (b, c) isochrons based on isotopic studies of zircon and sphene: (b) from blastomylonitic matrix, (c) from migmatite blocks.

U–Pb isotope data on zircons and sphenes from rocks of the tectonic mélange sequence recovered by Borehole North Molokovo

No.	Fraction, μm	Weight, g	Content, ppm		Pb isotopic composition			Isotopic ratios and age, Ma		
			U	Pb	²⁰⁶ Pb/ ²⁰⁴ Pb	²⁰⁶ Pb/ ²⁰⁷ Pb	²⁰⁶ Pb/ ²⁰⁸ Pb	²⁰⁶ Pb/ ²³⁸ U	²⁰⁷ Pb/ ²³⁵ U	²⁰⁷ Pb/ ²⁰⁶ Pb
Borehole North Molokovo										
1	Zircon + 100	0.0023	97.6	57.34	1600	5.8377	2.994	0.4499	10.1488	2493.2 ± 3.1
2	Zircon –100 + 75	0.0022	102.5	58.32	3125	5.9913	3.099	0.4423	9.9416	2487.3 ± 2.3
3	Zircon –75	0.0021	98.00	53.36	6670	6.0775	3.071	0.4243	9.5236	2484.8 ± 2
4	Sphene	0.005	15.93	8.098	112.1	4.381	2.443	0.3121 1750.9	4.6076 1750.7	1750.3 ± 13
Borehole Nevskaya-184										
1	Zircon –45	0.0013	2319	78.8	466	7.985	4.829	0.02871	0.385	1541 ± 2.3
2	Zircon + 75	0.0013	436.5	24.5	434	7.600	5.151	0.0483	0.666	1625 ± 1.8
3	Zircon –75, Ñ.Đ.	0.003			103	4.256	2.233	0.1914	2.684	1656 ± 12
Parameters and measurement results					Borehole					
					North Molokovo			Nevskaya-184		
Procedure blank (ng Pb)					0.2			0.3		
Equipment for measuring the isotopic composition					TSN 206A 1-channel solid-phase mass spectrometer (Cameca)			TRITON multichannel solid-phase mass spectrometer		
Correction for the common Pb admixture introduced in line with the model (Stacey and Kramers, 1975) for age (Ma)					for zircons – 2450 for sphenes – 1750			1980		
Error in U–Pb (%)					0.5			0.3		
Isotopic age of zircons based on the upper intercept of discordia with concordia (Ma)					2496 ± 9.2			1660 ± 32		
Isotopic age of sphene (Ma) concordant with isotopic ratios					1750 ± 10			—		

Note. sphene extracted from biotite-amphibole gneisses that form mélange matrix (sample SM-2, specimen 31/4, 70–86; depth interval 3237–3249 m). Zircon extracted from massive blocks of migmatites (sample CM-3, specimens 32/1, 12–20; 32/3, 40–50; 32/4, 70–86; depth interval 3297–3303 m).

Blastomylonites occur in the entire interval of 3210–3313 m. In terms of lithological composition, they are represented by dark to light gray and pinkish coarse-grained biotite–amphibole gneisses with the granoblastic and lepidogranoblastic textures (Fig. 2). Rock density varies from 2.3 to 3.1 g/cm³. They are characterized by the thin (a few millimeters) parallel-banded structure grading into the discrete or lenticular variety in some places. Dark-colored bands are thickened up to 1 cm in some places. The bands are usually oriented at 45° to the core axis. Relicts of the primary rock are represented by porphyroclasts of the altered potassic feldspars and plagioclases similar to their counterparts in migmatites. The rocks demonstrate characteristic features of mechanical pressure and heating. This is reflected in the development of foliated and augen structures, destruction of large grains with the formation of mosaic textures, and recrystallization.

They contain quartz (25–35%), feldspars (25–35%), hornblende (10–20%), biotite (20–30%), epidote (up to 10%), and sphene (up to 5–10%).

Accessory minerals are dominated by apatite and zircon.

Feldspars are usually dominated by potassic minerals (orthoclase and microcline). In porphyroclasts, they are usually pelitized, sericitized, and perthitized. Newly-formed minerals are represented by microcline, which are abundant both in porphyroblasts (up to 2 cm) and groundmass. Crystals of the newly-formed microcline are unaltered and lacking microinclusions. In gneisses subjected to microclinization, the quartz content increases up to 40%, and some of its grains are faceted. Both fresh and altered hornblende crystals occur in association with biotite.

Blastomylonites contain abundant epidote. The latter is present as euhedral (frequently zoned) crystals spatially confined to amphiboles and biotite (Fig. 2). Rounded or strongly corroded relicts of these minerals are frequently enclosed in epidote crystals. At contacts with quartz and plagioclase, epidote is characterized by sinuous boundaries. Such a relationship indicates the following succession in crystallization: (hornblende + biotite)–epidote–(quartz + feldspar). A

similar mineral association, in which epidote behaves as a late magmatic mineral, was established in some postcollisional granitoids and obtained by the experimental melting of synthetic granodiorite (Zen and Hammastrom, 1984). Therefore, the temperature of this process can be estimated at 680–710°C.

Sphene is usually developed crystal clusters along the amphibole periphery. However, it is also frequently represented by individual rhomboid crystals. Correspondence of the isotopic composition of sphene to concordia indicates that the latter represents a newly formed mineral with the isotopic signature completely rejuvenated (developed) due to a tectonomagmatic event 1750 ± 10 Ma ago (Fig. 2b). The closure temperature of the U–Pb system in sphene corresponds to 650–700°C, which determines the lower temperature limit of blastomylonite formation. Taking the mineral composition of rocks into consideration, one can assume that blastomylonites were formed at a temperature ranging from 700 to 750°C (Chamov, 2005).

Migmatites are established in the depth intervals of 3285–3303 and 3309–3311 m, where they are represented by the dominant massive coarse-grained pinkish gray rocks with large (up to 2.5 cm) porphyroblasts of feldspars (microcline and plagioclase) (Fig. 2). The rock density varies from 2.6 to 3.15 g/cm³. The rocks have an augen (locally banded) structure similar to that in blastomylonites. Areas with the massive texture frequently demonstrate the pinching out (degeneration) of lenticular dark-colored aggregates. The interval of 3300.2–3300.5 m encloses a steep to vertical contact between spotty migmatite and banded blastomylonite slightly flattening downward the section. The contact is accompanied by aggregates of dark gray rock components, which form a continuous well-developed (approximately 1 cm thick) boundary suture. Coarse and discrete banded patterns in blastomylonites are also related to the segregation of dark-colored components. Bands are oriented at approximately 30° to the core axis and 25°–30° to the contact, along which they degenerate, become oriented parallel to dark-colored aggregates of the boundary suture, and do not continue in migmatites.

Migmatites are characterized by the granoblastic texture. They are composed of quartz (25–40%), feldspars (30–40%), hornblende (10–15%), biotite (up to 25%), sphene (5–10%), and chlorite (up to 10%). Accessory minerals are represented by apatite, zircon, sphene, anatase, and chlorite. Garnet and ore minerals (ilmenite?) occur as single grains. The epidote content in migmatites is substantially lower relative to that in blastomylonites.

Two generations of potassic feldspars are defined. The primary potassic feldspar is subjected to albitization, while the secondary variety of metasomatic origin is represented by microcline mostly confined to porphyroblasts. Plagioclases of the albite–oligoclase composition prevail in the groundmass. Dark-colored minerals (hornblende and biotite) form areas with the gneissoid and foliated structures. One can see milky white quartz veins (several centimeters thick) with hematite and ore (sphene–anatase) association at the contact. Some quartz grains are faceted.

Wide development of granoblastic textures in the migmatite groundmass indicates their formation owing to melting. At the same time, the presence of faceted grains, occurrence of two generations of feldspars, and development of ore (sphene–anatase) association reflect a substantial influence of metasomatic processes on the formation of the rock appearance.

Occurrence of dark-colored bands and lenses in massive structures points to plastic deformations of the rock. Widely developed cataclasis was superimposed on the older brittle rocks.

The isotopic age of zircons from these rocks based on the upper intercept of discordia with concordia ranges from 2488 ± 9 to 2496 ± 9.2 Ma, which corresponds to the protolith formation period (Figs. 2b, 2c).

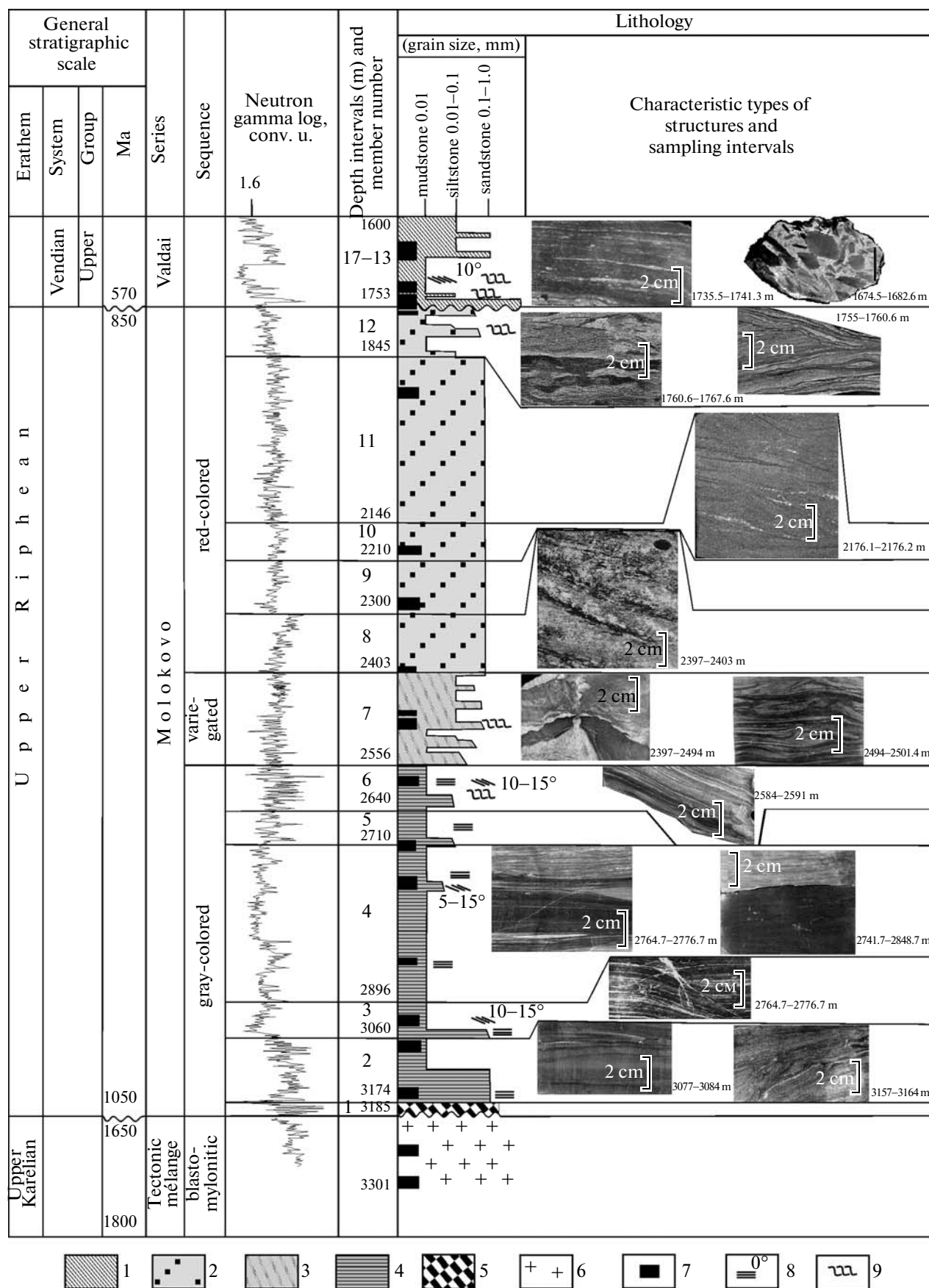
In terms of the chemical composition, both migmatites and blastomylonites belong to granitoid rocks related to collisional processes. In the geodynamic diagram (Batchelor and Bowden, 1985), their data points form a continuous “cloud” extended from the field of preplate collision to the field of postcollisional uplift (Fig. 2a). Since data points in this “cloud” (Fig. 2a and other diagrams) overlap each other and show no trend during the transition from migmatites to blastomylonites, one can assume that dynamometamorphism, which resulted in blastomylonitization, was isochemical.

MOLOKOVO GROUP (UPPER RIPHEAN ERATHEM)

The Molokovo Group comprises all sedimentary complexes sandwiched between metamorphic rocks of the basement and Upper Vendian sedimentary rocks in the interval of 1753–3185 m (Fig. 3). The group includes three sequences with characteristic features that are readily recognized in core: lower gray-colored, transitional variegated, and upper red-colored.

The *gray-colored sequence* unites rocks in the depth interval of 2556–3185 m and includes six members largely composed of gray to dark gray fine-grained rocks.

Fig. 3. Characteristics of the North Molokovo parametric borehole section. (1–5) Facies: (1) marine sediments, (2) red-colored sandy sediments of intermontane troughs, (3) variegated sandy–silty–clayey sediments of shallow lakes, (4) gray-colored sandy–silty–clayey sediments of deep lakes, (5) coarse–detrital sediments of fault-line depressions; (6) basement; (7) sampled core intervals; (8) bedding inclination; (9) slump structures.



Member 1 (interval 3174–3185 m, thickness 11 m) was not cored. Based on the complex interpretation of GIS materials obtained by specialists from the Tver’geofizika Scientific–Industrial Center, this interval is composed of incoherent coarse-detrital rocks. The borehole is characterized by intense destruction of walls with the formation of caverns >0.3 m in diameter.

This conclusion is consistent with the results obtained for other boreholes, where the basal part of the sedimentary cover encloses beds composed of basement rock fragments (Anatol’eva, 1972).

Member 2 (interval 3060–3174 m, thickness 114 m) is represented by alternating silty mudstones, thin-bedded sandstones, and gray clayey siltstones. The dark gray (locally brownish) silty mudstones are characterized by thin horizontal and wavy bedding. The sandstones have gray to greenish gray color and fine-grained to inequigranular structure. The number and thickness of sandstone beds increases toward the base of the member. The rocks are characterized by large-scale cross bedding.

The mudstones are silty with the microlaminated thin horizontal bedding. The beds enriched in silty material are 0.1 to 0.2 m thick. Clasts are largely represented by quartz and feldspars. Silty and pelitic micaceous detritus is arranged parallel to bedding surfaces. Accumulations of fine-grained pyrite are present. The mudstones have clayey, micaceous, and low-carbonate composition with the feldspar–quartz admixture. Sorting is moderate. The structure is microlaminated and thin horizontal-wavy. Micaceous detritus is oriented parallel to bedding surfaces. The rock has clayey, interstitial-basal hydromica–mica–chlorite–kaolinite, interstitial kaolinite, and corrosional calcite cement. The sandstones have silty (gravelly in some places) and feldspar–quartz composition (arkosic at the base of the member). Clastic material is poorly sorted (locally unsorted) and subangular, with an insignificant admixture of subrounded grains. Clastic material is composed of quartz (60–90%), feldspars (5–30%), muscovite (up to 5%), and partly chloritized biotite (up to 5%). Gravel-sized clasts are represented by granitoids.

Accessory terrigenous components in the heavy fraction include epidote (up to 18%, 65% in samples from the basal part of the member), ore minerals (up to 15%, 32% in samples from the middle part of the member), zircon (up to 19%), leucoxene (up to 21%), garnet (up to 16%), and tourmaline (up to 11%). Sphene, amphibole, and rutile occur as single grains. Morphology of detrital epidote from the heavy fraction of sedimentary rocks and its chemical composition determined by the microprobe method are identical to those in metamorphic rocks from the upper part of the basement (Chamov et al., 2003). Fragments of epidote crystals in sedimentary rocks of Member 2 are lacking signs of dissolution or rounding and they

retain distinct facets typical of euhedral crystals in blastomylonites.

The X-ray structural analysis of oriented samples of the bulk fraction from mudstones and sandstones revealed the presence of quartz, feldspar, calcite, kaolinite, and two micaceous minerals (dioctahedral mica with single swelling layers and hydromica).

Samples from the middle part of the interval of 3164–3157 m yielded the following acritarchs: *Leiosphaeridia atava* (Naum.) emend. Jank., *tenuissima* Eisenack, *L. jacutica* (Tim.) emend. Mikh. et Jank., *L. sp. 1* (“fissionable” sheaths), *Nucellosphaeridium nordium* (Tim.), *Spumosina rubiginosa* (Andreeva). *Leiosphaeridia* representatives are medium- to large-sized, mostly thin-walled (up to 200–220 µm). One can also see sheaths with internal bodies (300–320 µm) and single fragments of more compact spumosins (up to 320 µm).

Member 3 (interval 2896–3060 m, thickness 164 m) is composed of mudstones with rare siltstone interbeds. The mudstones are dark gray to gray, silty, with an insignificant sand admixture in basal part of the member. Bedding is vague, discontinuous, horizontal, or lenticular. Bedding is distinct, parallel-horizontal, and thin gentle wavy in beds enriched in silty or sandy material. One can see frequent alternation of mudstones and siltstones. In some intervals of the section, horizontal bedding is inclined at 10°–15° to the horizontal plane.

The mudstones with the silty admixture up to 10–50% are carbonatized in some places. The structure is vague, microlaminated, horizontal, discontinuous, and micrograded. Clastic material is represented by quartz and single feldspar grains. Fine micaceous detritus is oriented parallel to bedding surfaces. The siltstones have micaceous–clayey feldspar–quartz composition. Sorting is moderate. The microlaminated structure is related to alternation of silty (up to 4.5 mm) and micaceous–clayey (0.1–2.5 mm) laminae with a low silt admixture. The rock has clayey interstitial-basal (locally regenerated quartz) cement with the late corrosional calcite. The rocks are slightly pyritized.

Accessory terrigenous minerals of the heavy fraction (single grains) are represented by garnet, tourmaline, zircon, leucoxene, ore minerals, apatite, and epidote.

The X-ray structural analysis of oriented clay samples (fraction <0.001 mm) from siltstones and mudstones revealed kaolinite, traces of defective chlorite, and two micas (mixed-layer illite–smectite and dioctahedral mica with single swelling layers).

Member 4 (interval 2710–2896 m, thickness 186 m) is composed of mudstones. They occur as dark gray to gray (locally with bluish or greenish tint) massive calcareous rocks with a variable silty admixture (5–50%) and vague discontinuous horizontal or lenticular bedding. One can often see thin alternation of

mudstones and clayey siltstones. Bedding is very thin, parallel, and discontinuous-horizontal (with laminae 1–2 mm thick) in some places. In some intervals of the section, horizontal bedding surfaces are inclined at angles up to 10°–15°, indicating the intermittent inclination of the basin bottom. The rocks are slightly pyritized. Mudstones enclose interbeds of dark gray massive secondary limestones.

The clastic material is represented by feldspars and quartz. The fine-grained micaceous detritus (up to 50%) is oriented parallel to bedding surfaces. The rocks are characterized by microlaminated-horizontal and lenticular structure accentuated by a silty and micaceous material. Lenses and microlaminae are 0.2–0.5 mm thick. Silty laminae and microlenses include the basal clayey or corrosional calcite cement. The groundmass contains authigenic fine-grained pyrite.

Accessory terrigenous minerals of the heavy fraction (single grains) are garnet, tourmaline, zircon, leucocoxene, ore minerals, apatite, and epidote.

The X-ray structural analysis of oriented clay samples (fraction <0.001 mm) from siltstones and mudstones revealed kaolinite, traces of defective chlorite, and two micas (mixed-layer illite–smectite and dioctahedral mica with single swelling layers).

The lower part of the interval of 2848–2841 m contains microfossils (acritarchs): *Leiosphaeridia minutissima* (Naum.) emend. Jank., *L. atava* (Naum.) emend. Jank., *L. tenuissima* Eisenack, *L. sp. 1* (“fissionable” sheaths), *Navifusa majensis* Pjat. Remarkable among them are large thin-walled spheroid morphotypes, *Leiosphaeridia* representatives united into diads or triads and having a hollow in common (up to <300 µm in diameter), and ellipsoid *Navifusa* forms (340 × 240 µm).

Complex forms are represented by single *Pellicularia* sp. (filmy fusiform structures 100–150 × 30–40 µm in size).

The middle part of the interval of 2776–2764 m yielded the following acritarchs: *Leiosphaeridia minutissima* (Naum.) emend. Jank., *L. atava* (Naum.) emend. Jank., *L. tenuissima* Eisenack, *Nucellosphaeridium nordium* (Tim.), *Spumosina rubiginosa* (Andreeva). The assemblage is dominated by medium- to large-sized (100–150, rarely 200–220 µm across) compact to thin-walled specimens. Discoid spumousins (up to 200 µm in size) almost opaque in the transmitted light are particularly abundant.

The complex acritarchs include different forms: *Caudosphaera expansa* Herm. et Tim., which represent sheaths with a long process sometimes complicated by vague branching (the main body is 100 × 120 µm across, while the process is up to 200 µm long and 40 µm wide); *Germinosphaera* sp., drop-shaped fossils with a small process (sheath up to 200 µm across, process up to 50 µm long); and *Palaeovaucheria* cf. *clavata* Herm., a rare component of Late Riphean microbio-

tas representing moniliform branching thaloms with swellings; several specimens (up to 500 × 50 µm in size) with clearly widened bodies but lacking septae; *Majasphaeridium* sp., very large sacciform irregular structures (up to 300–500 µm across) connected by processes with rounded or asymmetrical sheaths; and reproductive organs of mushroom-like organisms.

Member 5 (interval 2640–2710 m, thickness 70 m) is composed of dark gray silty mudstones (locally carbonatized) with vague discontinuous horizontal lenticular-bedded or massive structure. In beds enriched with silty or sandy material, bedding is distinct, parallel, horizontal, and small-scale flattened wavy. The member demonstrates slickensides inclined up to 45° to the core axis.

The mudstones have microlaminated horizontal structures accentuated by silty material. Silty laminae are usually carbonatized. The content of clastic silty feldspar–quartz material is usually up to 5% and up to 50% in some microlaminae. The structure is chaotic to microlaminated. Sorting of detrital material is medium to good. The cement is composed of the basal-interstitial clayey (locally regenerated quartz) material. The youngest corrosional calcite cement is also observed in some places.

Accessory terrigenous minerals of the heavy fraction (single grains) are represented by garnet, tourmaline, zircon, leucocoxene, ore minerals, apatite, and epidote.

The X-ray structural analysis of oriented clay samples (fraction <0.001 mm) from siltstones and mudstones revealed kaolinite, traces of defective chlorite, and two micas (mixed-layer illite–smectite and dioctahedral mica with single swelling interlayers).

The middle part of the interval of 2710–2700 m yielded the following microfossils (acritarchs): *Leiosphaeridia atava* (Naum.) emend. Jank., *L. tenuissima* Eisenack, *Nucellosphaeridium nordium* (Tim.), *Spumosina rubiginosa* (Andreeva), *Konderia elliptica* A. Weiss. Numerous sheaths are dominated by thin-walled varieties. Most of them are >200 µm across. Some *Leiosphaeridia* and *Konderia* representatives are >300 µm in size.

Complex forms are represented by *Pseudotawuia* sp., bean-shaped large (up to 320 × 160 µm) specimens with the inner sheath in each widened segment repeating outlines of the outer one.

Member 6 (interval 2556–2640 m, thickness 84 m) is represented by alternating gray to dark gray silty mudstones, lighter greenish gray to gray clayey micaceous siltstones, and fine-grained silty sandstones with individual beds up to 2 cm thick. The distribution of different grain-size rock minerals in the member is irregular: some layers (up to 1.5–2.0 m thick) are dominated by mudstone, while others are represented by siltstone and sandstone. The member is characterized by horizontal parallel, discontinuous small-scale

lenticular, or less common cross-wavy and small-scale cross bedding.

The mudstones have silty (chlorite—hydromica—mica—kaolinite) composition. The content of silty feldspar—quartz material in the groundmass amounts to 25%. Micaceous detritus (>50%) is arranged parallel to bedding surfaces. The rock has microlaminated horizontal structure due to the occurrence of thin microlaminae enriched in silty material. The rocks are slightly pyritized.

The siltstones are characterized by micaceous and clayey—calcareous feldspar—quartz composition and vague microlaminated structure accentuated by accumulations of micaceous detritus. Sorting and roundness of detrital material are poor. The cement is composed of the interstitial-basal clayey (hydromica—chlorite—kaolinite) and the youngest calcite materials.

The sandstones have feldspar—quartz and calcareous compositions with a variable amount of the clay admixture. Sorting degree varies from medium to low. Roundness of detrital material is poor. The rock also contains subrounded sand-sized quartz grains. The microlaminated horizontal-wavy to cross-wavy discontinuous structure is emphasized by accumulations of micaceous material. Detrital material is represented by quartz (80–85%), feldspars (10–15%), chloritized biotite (up to 10%), muscovite (single flakes), and rare fine-grained sericite detritus. Cement is represented by clayey interstitial and basal-interstitial chlorite—hydromica—kaolinite (locally quartz) material regenerated due to the pressure dissolution of mineral grains). Corrosional carbonate is the youngest cement.

Accessory terrigenous minerals of the heavy fraction (single grains) are observed as leucoxene, ore minerals, tourmaline, apatite, garnet, zircon, and sphene.

The X-ray structural analysis of oriented clay samples (fraction <0.001 mm) from the cement of sandstones revealed kaolinite with traces of dickite, defective chlorite, and two micas (mixed-layer illite—smectite and dioctahedral mica with single swelling interlayers).

The lower part of the interval of 2591–2584 m contains the following microfossils (acritarchs): *Leiosphaeridia atava* (Naum.) emend. Jank, *L. tenuissima* Eisenack, *L. bicrura* Jank., *L. sp. 2* (accumulations of sheaths), *Chuarina circularis* Walcott emend. Vidal, Ford, *Ch. globosa* Ogurtz. et Serg., *Nucellosphaeridium nordium* (Tim.), *Pterospermopsimorpha insolita* Tim. emend. Mikh., *P. pileiformis* Tim. emend. Mikh., *Aimia sp.* Large (mostly thin-walled) sheaths are particularly abundant. The dominant size of specimens is 200–260 µm for *Leiosphaeridia*, up to 440 µm for *Chuarina*, up to 280 µm for varieties with internal bodies, and up to 300 µm for forms with the median fracture of the sheath.

Filamentous forms and akinets include *Asperatofilum experatus* (Herm.) (chagrin tubular sheaths 40–50 µm

wide) and *Brevitrichoides bashkiricus* Jank. (widely rounded ellipsoid bodies 240 × 60 µm in size).

The complex varieties are represented by *Pellicularia sp.*—thin-walled fusiform fossils that are strongly deformed and corroded (200–250 × 40–60 µm in size).

The *variegated sequence* unites gray-colored and red-brown rocks in the interval of 2403–2556 m and is represented by a single member.

Member 7 (interval 2403–2556 m, thickness 153 m) consists of alternating brown and gray, medium- to fine-grained, micaceous—clayey siltstones (less commonly, brown mudstones with a high silty content). Some layers contain intraclasts of brown-red mudstone. The sandstones and siltstones are characterized by horizontal, small-scale wavy, cross-wavy, and rare small-scale cross bedding. Alternating beds are from 1 to 15 cm thick. Alternation of beds demonstrates lenticular patterns in some places. The member is characterized by the occurrence of small-scale structures of underwater slumping. The rocks show syndimentary fissures.

The silty mudstones have chlorite—hydromica—kaolinite composition. The content of detrital silty feldspar—quartz material varies from 5–15 to 25–30%. Their structure is microlaminated horizontal with laminae 0.3–0.5 mm thick. The rock is red-brown owing to the admixture of iron oxides in the groundmass.

Siltstones have micaceous—clayey feldspar—quartz composition. Sandstones have arkosic calcareous (less commonly, feldspar—quartz) composition. Detrital material represented by subrounded to angular mineral grains is moderately sorted. It is composed of quartz (60–85%), feldspars (10–30%) chloritized or partly decomposed up to iron oxides biotite (5–15, rarely 20–30%), and muscovite (1–5%). The sandstones contain regenerated quartz cement related to the pressure dissolution of grains (conformal-regeneration structures). Interstitial kaolinite and filmy hydromicaceous cement are less common. The basal-interstitial corrosional calcite cement represents the youngest generation. The siltstones demonstrate the development of interstitial kaolinite and youngest corrosional cement.

Accessory terrigenous minerals of the heavy fraction are as follows: leucoxene (27%), zircon (up to 19%), tourmaline (up to 18%), apatite (up to 12%), garnet (up to 7%), amphibole (up to 7%), ore minerals (up to 5%), epidote (up to 5%), and rutile (single grains).

The X-ray structural analysis of oriented clay samples (fraction <0.001 mm) from the cement of sandstones revealed two micas: mixed-layer illite—smectite (with 20–30% of smectite packets) and dioctahedral mica (with single swelling interlayers). In addition, the mixed-layer (chlorite—swelling chlorite) structure and kaolinite were established.

The middle part of the interval of 2494–2487 m yielded acritarch species *Leiosphaeridia minutissima* (Naum.) emend. Jank. Small strongly corroded sheaths (up to 60 μm in diameter) are rare.

The *red-colored sequence* unites mainly red and red-brown (with violet tint) rocks in the interval of 1753–2403 m. The sequence consists of five members (Fig. 3).

Member 8 (interval 2300–2403 m, thickness 103 m) is composed of red-brown, fine- to medium-grained and inequigranular sandstones with an insignificant gravelly admixture in some places. The rocks are characterized by massive or unidirectionally oriented cross bedding, with beds up to 10–15 cm thick and inclined at up to 65° to the core axis. Dark brown clayey admixture slightly increases upward the section and thin (1–3 mm) laminae of clayey sandstone appear in oblique layers up to 1.5–2.0 cm thick. The basal part of the member contains single intraclasts (0.9 \times 0.6 cm in size) of well-rounded flattened compact dark brown mudstone with a low silty admixture.

The sandstones occur as arkosic, inequigranular, poorly sorted, medium- to fine-grained rocks with a low clay admixture. Subrounded to angular detrital material is represented by quartz (60–70%), feldspars (20–30%), partly chloritized biotite flakes, and rare small muscovite flakes. Pores are partly filled with the well-crystallized kaolinite and subordinate calcite. Some grains have a thin illite–smectite crustification coating. The sandstones are brown-colored owing to the iron hydroxide coating on detrital grains.

Accessory terrigenous minerals of the heavy fraction are represented by zircon (up to 45%), leucoxene (30%), garnet (up to 10%), tourmaline (up to 12%), and ore minerals (up to 5%), as well as single epidote, amphibole, sphene, rutile, and apatite grains.

The X-ray structural analysis of oriented clay samples (fraction <0.001 mm) from the cement of sandstones revealed kaolinite, mixed-layer chlorite–smectite (with 65–70% of chlorite), and two mica phases (mixed-layer illite–smectite and dioctahedral mica with single swelling interlayers).

Member 9 (interval 2210–2300 m, thickness 90 m) is represented by uniform lilac-brown inequigranular, poorly sorted, massive (usually almost incoherent) sandstones with gravel and insignificant clay admixture. The grain-size composition of detrital material is highly variable and characterized by gradual transitions in the section. No distinct bedding surfaces are observed. The upper part of the member (interval 2270–2271 m) encloses sandstones with vague small-scale oblique striated bedding resembling that in the overlying Member 10. The member is characterized by secondary spotty patterns. Chaotically scattered leaching spots (from 1 to 7 cm across) are largely confined to more loose and less clayey medium- to fine-grained sandstones.

The sandstones have arkosic and feldspar–quartz composition. Subrounded to angular detrital material is represented by quartz (60–75%) and feldspars (10–30%) with subordinate muscovite and chloritized biotite flakes, single intraclasts of brown mudstones, and fragments of strongly altered basic volcanics. Cement is poorly developed. Pores are partly filled with the well-crystallized kaolinite or the youngest calcite. Some grains have a thin illite–smectite crustification coating. Brown color of sandstones is related to the wide development of iron hydroxide films on detrital grains.

Accessory terrigenous minerals of the heavy fraction are represented by zircon (up to 35%), leucoxene (up to 30%), garnet (up to 10%), tourmaline (up to 12%), and ore minerals (up to 14%), as well as single amphibole, sphene, rutile, and apatite grains.

The X-ray structural analysis of oriented clay samples (fraction <0.001 mm) from the cement of sandstones revealed kaolinite, mixed-layer (chlorite–swelling chlorite) structures, and two mica phases (mixed-layer illite–smectite and dioctahedral mica with single swelling interlayers).

Member 10 (interval 2146–2210 m, thickness 64 m) consists of brown or dark gray, fine-grained, silty and clayey sandstones with horizontal wavy, small-scale striated, and cross-wavy bedding alternating with micaceous–clayey siltstones with distinct horizontal and wavy bedding accentuated by the sandy admixture. Thickness of rhythms decreases downsection from 10–20 to 3–5 cm. The sandstones contain rare accumulations of small (up to 1 cm) clasts of brown or dark gray siltstone (up to 30%). In oblique laminae (>7.5 cm long), the height of waves varies from 0.5 to 3 cm. Transition between sandstones and siltstones is sharp (locally gradual) and rapid.

The siltstones are marked by feldspar–quartz composition with significant clay admixture, while sandstones consist of feldspars and quartz. The poorly sorted detrital material is represented by quartz (up to 70%), feldspars (up to 20%), large chloritized biotite flakes (up to 10%), and numerous small mica detritus. Cement is composed of the interstitial-basal and basal clayey kaolinite–hydromica–chlorite material.

The X-ray structural analysis of oriented samples of the bulk sandstone fraction revealed quartz, feldspars, chlorite, kaolinite, and two mica phases (dioctahedral mica with single swelling interlayers and hydromicas).

Member 11 (interval 1845–2146 m, thickness 301 m) is composed of brown sandstones with nests of light gray material. In some layers, sandstones are light gray, poorly to moderately sorted, largely fine- to medium-grained, weakly cemented, and massive with insignificant clay admixture. The sandstones are variably lithified in the section.

The sandstones have feldspar–quartz composition with subrounded detrital material represented by quartz (80–85%), feldspars (>10%), and mudstone

lithoclasts (3–5%). The filmy hydromicaceous cement is poorly developed. Some pores are filled with crystallized kaolinite or the youngest calcite.

Accessory terrigenous minerals of the heavy fraction are represented by leucoxene (up to 46%), garnet (up to 19%), zircon (up to 17%), tourmaline (up to 10%), and ore minerals (up to 8%), as well as single sphene grains.

The X-ray structural analysis of oriented clay samples (fraction <0.001 mm) from the cement of sandstones revealed the development of two mica minerals (mixed-layer chlorite–smectite with 35–40% of swelling interlayers and hydromicas with 5–10% of swelling interlayers), well-crystallized kaolinite, swelling chlorite, and, presumably, traces of chlorite–smectite.

Member 12 (interval 1753–1845 m, thickness 92 m) is represented by irregularly alternating brown and gray, medium- to fine-grained, silty (frequently micaceous) sandstones with an insignificant clay admixture and micaceous–clayey siltstones. Thickness of the grain-size variable beds ranges from 1 to 15 cm; thickness of color-variable interlayers, from 0.5 to 3 m. Brown-red mudstone rolls occur in some places. The rocks are characterized by horizontal, small-scale wavy, cross-wavy, and local small-scale cross bedding. Small-scale underwater slump structures are noteworthy.

The siltstones are marked by clayey–micaceous feldspar–quartz composition, while the sandstones are characterized by feldspar–quartz (arkosic at the base of the member) calcareous composition. Sub-rounded and angular detrital materials are moderately sorted. Detrital material of sandstones is represented by quartz (60–85%), feldspars (10–30%), partly chloritized, kaolinitized, or decomposed up to iron hydroxides biotite (5–15%, 20–30% in some places), and muscovite (1–5%). The regenerated quartz cement is related to the pressure dissolution of grains (conformal-regeneration textures). Some pores are filled with kaolinite. Interstitial-basal and filmy hydromicaceous cement is poorly developed. Corrosional calcite is the youngest cement. Secondary structures in sandstones are represented by acicular illite–smectite developed along peripheral parts of detrital grains and in cement.

Accessory terrigenous minerals of the heavy fraction are represented by leucoxene (up to 27%), zircon (up to 19%), tourmaline (up to 18%), apatite (up to 12%), garnet (up to 7%), amphibole (up to 7%), ore minerals (up to 5%), and epidote (up to 5%), as well as single rutile grains.

The X-ray structural analysis of oriented clay samples (fraction <0.001 mm) from the cement of sandstones revealed the development of mixed-layer chlorite–smectite (with 20–30% of swelling interlayers), dioctahedral mica (with single swelling interlayers), mixed-layer chlorite–swelling chlorite aggregates, and kaolinite (traces).

Valdai Group (Upper Vendian System)

The Upper Vendian sedimentary succession is divided into five members (from the bottom to top): Member 13 (pebbly–gravelly sandstones, interval 1750.5–1753.0 m), Member 14 (sandy mudstones, 1720.0–1750.5 m), Member 15 (mudstones, 1685–1720 m), Member 16 (sandstones, 1662–1685 m), and Member 17 (clayey–silty, 1600–1662 m). Members 13, 14, and 16 are sufficiently well characterized by core material, while members 15 and 17 are defined conditionally.

The sequence is composed of the following sediments: greenish gray, fine- to medium-grained clayey, poorly to moderately sorted sandstones and siltstones with the horizontal, wavy, and small-scale striated bedding and slump structures; dark gray, horizontally bedded mudstones; and clayey siltstones with sandstone interbeds. Some intervals demonstrate distinct discontinuous horizontal, horizontal-wavy, lenticular, and small-scale (mutually truncating and differently oriented) cross bedding and interbeds of intraformation breccia. The basal part of the sequence includes light gray or greenish, poorly sorted clayey, massive sandstones with inclusions of gravel and pebbles, as well as small boulders of quartz, sedimentary rocks, and volcanics. Pebbles are scattered chaotically and differently rounded: small rock fragments are usually angular, while large pebbles are isometric or flattened.

In terms of mineral composition, the sandstones largely represent oligomictic feldspar–quartz, arkosic, and less common monomineral quartzose rocks. The siltstones are marked by feldspar–quartz composition. The mudstones are composed of silty, chlorite–hydromica, and mica–kaolinite material with illite–smectite admixture in some places.

COMPOSITION AND STRUCTURE OF THE REFERENCE SECTION

Facies Composition of Sedimentary Rocks

The study of textural–structural features of sedimentary rocks recovered by drilling made it possible to define the facies types of sediments accumulated in different marine and continental settings.

Valdai Group. The textural–structural features of sediments of this group imply their deposition in a large basin away from the coast in low-energy hydrodynamic conditions (members 17, 14), in open shallow-water settings with relatively high-energy hydrodynamics (Member 16), and in the coastal zone (Member 13).

Molokovo Group. Despite apparent lithofacies differences, sedimentary sequences of this group were most likely formed during a single development stage of the region. With regard to their tectonic settings, all three sequences reflect a single geodynamic process, different phases of which resulted in substantial changes of sedimentation conditions.

Three facies types of sediments are defined in the section of gray-colored and variegated sequences.

The facies of fault-line depressions unites variegated breccia-conglomerates with the sandy-clayey matrix and interbeds of variegated siltstones, mudstones, and inequigranular (unsorted and poorly sorted) sandstones frequently grading into breccia and breccia-conglomerates. Large fragments are represented by metamorphic rocks of the basement, which constitute surrounding parts of the basin base. Such properties of sedimentary material are typical of landslide sediments, which are deposited in structural traps along tectonic scarps. Variegated coloration of sediments implies subaerial settings of their accumulation. Sediments of this facies are confined to the interface of gray-colored sequence and basement.

The facies of shallow lakes is represented by irregularly alternating dark gray (locally brown) silty mudstones and gray (poorly sorted) siltstone enclosing lenses and interbeds of light gray, poorly sorted, medium- to fine-grained sandstone with an insignificant clay admixture. Sediments of this facies are characterized by thin lenticular, horizontal, gentle and wavy (frequently discontinuous) cross bedding. One can also see small-scale structures of underwater slumping. Structural features indicate that sediments of the facies accumulated on mobile shoals with an unstable hydrodynamic regime. Brown color of rocks points to subaerial sedimentation settings of this facies. Toward axial parts of sedimentary basins, the sediments grade into the facies of deep lakes. Similar transition is also observed in the vertical section. Sediments of the facies are established at the base and top of gray-colored sections in each of the troughs, suggesting a transgressive-regressive trend in sedimentation. In addition, sediments of the facies are confined to tectonic scarps in the near-slope part of troughs near the coarse-detrital sediments of fault-line depressions. Thickness of the facies varies from 50–360 to 70–490 m at the southwestern and northeastern flanks of the aulacogen, respectively.

The facies of deep lakes is composed of gray to dark gray mudstones with variable silt admixture and gray siltstones with subordinate interbeds of moderately to poorly sorted, medium- to fine-grained light gray sediments. Bedding is thin horizontal, locally discontinuous, gentle- and lenticular-wavy. Detrital material is subrounded to angular. The structural features of these rocks are typical of sediments deposited in central parts of deep basins under the influence of low-energy bottom currents (Reding et al., 1978). The lack of well-fractionated hemipelagic and pelagic clayey sediments, combined with the angular appearance and poor sorting of detrital material, suggest the lacustrine genesis of these sediments. Toward flanks of the basin, sediments of the facies are replaced by the coarser silty-sandy sediments of shallow lakes. In the East Mid-Russian segment of the aulacogen, thickness of these rocks increases from 120 m near the flank to

540 m in central parts of the basin and 2 km at the northeastern flank.

Two facies are distinguished in the red-colored sequence.

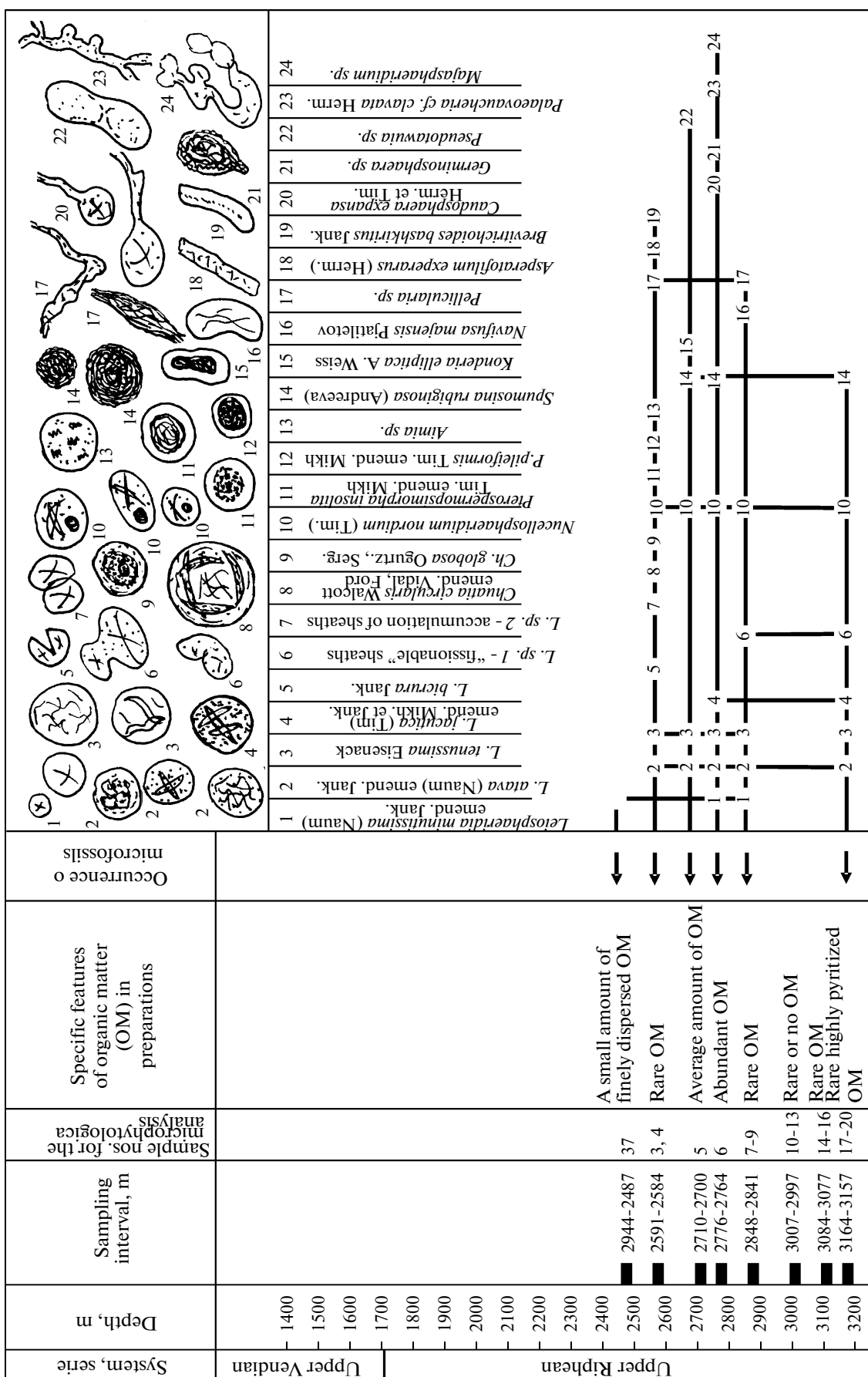
The facies of near-slope parts of intermontane troughs is represented by brown-red or lilac-brown, inequigranular unsorted, gravelly sandstones. One can also see poorly to moderately sorted sandstones with an insignificant clay admixture and large-scale unidirectional cross bedding. Fine-grained sandstones demonstrate small-scale striated cross lamination. The sediments are characterized the variable grain-size composition with gradual transitions between individual varieties. Coarse-detrital sediments are typical of slope bases (fans) of intermontane troughs. With regard to tectonics, this facies is similar to molasses. The sediments were accumulated at the terminal development stage of the Central Russia Aulacogen shear system, when partial inversion and appearance of local uplifts fostered an overcompensation regime in sedimentary basins, resulting in progradation of the coarse-detrital red-colored sediments from individual troughs and formation of a single spacious continental basin with alluvial-proluvial-lacustrine sedimentation. Shoaling of the basin is particularly well reflected in the southwestern direction. Thickness of sediments is approximately 200 m.

The facies of axial parts of intermontane troughs is composed of irregularly alternating, poorly sorted, red-brown medium- to fine-grained silty sandstones, micaceous siltstones, and mudstones. The sandstones and siltstones are characterized by horizontal, wavy, cross-wavy, and small-scale striated bedding and small-scale underwater slump structures. The sediments are genetically variable: even small core intervals demonstrate an association of alluvial and relatively calm-water sediments. Such conditions could develop in the central parts of intermontane troughs located away from their slopes. The formation and degradation of small lakes and intermittent channels could be provoked by block tectonic movements. The apparent thickness of sediments amounts to 400 m.

Microphytological Fossils in the Fine-Grained Varieties of Sedimentary Rocks from the Gray-Colored Sequence of the Molokovo Group

The interval of the section with microphytological remains (3164–2487 m) yielded a relatively impoverished assemblage of organic-walled forms (Fig. 4; members 2, 4–7 in the text). The assemblage includes more than 150 specimens of 16 genera and 17 species that differ in the structure of microfossils. Color index (from light yellow to dark orange) of the best-preserved organic-walled microfossils implies that the

¹ Data presented in this section are based on the results of joint studies (Chamov et al., 2003) edited by A.F. Veis.



← Fig. 4. Results of microphytological studies of Riphean sediments recovered by the North Molokovo parametric borehole.

host sequence was not subjected to intense thermal impact (no more than 80–100°C).

The considered microfossils occur at six stratigraphic levels and belong to a single assemblage. This is evident from similar preservation of all the examined specimens, universal prevalence of medium- to large-sized thin-walled acritarchs, and lack of a significant evolutionary trend in changes of their abundance and taxonomic diversity in the borehole section. The maximal diversity of microfossils is recorded in the middle part of the examined interval (2848–2584 m). The diversity decreases to three genera and five species in the lower part of this section (3164–3157 m) and a single species in the upper part (2494–2487 m).

The biostratigraphic analysis of the taxonomic composition of the established acritarch assemblage indicates the domination of the transit Late Proterozoic (Riphean) taxa: *Leosphaeridia minutissima* (Naum.) emend. Jank., *L. atava* (Naum.) emend. Jank., *L. tenuissima* Eisenack, *L. jacutica* (Tim.) emend. Mikh. et Jank., *L. bicrura* Jank., *Nucellosphaeridium nordium* (Tim.), *Pterospermopsimorpha insolita* (Tim.) emend. Mikh., *P. pileiformis* (Tim.) emend. Mikh., *Spumosina rubiginosa* (Andreeva), *Aimia* sp., and *Germinosphaera* sp.

The number of transit taxa in this assemblage exceeds that in the lower (3164–3157 m) and upper (2494–2487 m) parts of the section. Thus, based on the identified microfossils, one can only conclude that sequences corresponding to the basal and uppermost parts of the section correlate with the Riphean. Taking into consideration the additional secondary information on particularly large forms from these sediments and occurrence of specific “fissionable” (or monstrous) forms, host sequences may be attributed to the second half of the Riphean (Veis et al., 1988).

The assemblage from the middle part of the examined section (2848–2584 m) shows a substantially different composition. In addition to the transit taxa in the lower and upper parts, the acritarch assemblage includes large forms, such as *Chuarina circularis* Walcott emend. Vidal, Ford, *Ch. globosa* Ogurtz., Serg., *Konderia exuperatus* A. Weiss; *Navifusa majensis* Pjat.; tulubar sheaths *Asperatofulum exuperatus* (Herm.), ellipsoid structures representing probably akinetes *Brevitrichoides bashkircus* Jank., *Pseudotawuia* sp., sheaths with long processes (*Caudosphaera expansa* Herm. et Tim., branching thaloms with swellings (*Palaeovaucheria* cf. *clavata* (Herm.), fusiform filmy forms (*Pellicularia* sp., and *Majasphaeridium* sp. united by processes into aggregates.

In all of the scrutinized Riphean sections of the South Urals and Siberia with microphytological remains (Pyatiletov, 1988; Veis, 1988; Nagovitsyn, 2001; Veis and Vorob'eva, 2002), the morphotypes mentioned above are found in sediments attributed to

the Upper Riphean (based on biostratigraphic data). Only some of them (*Spumosina*, *Asperatofulum*, and others) are of the Vendian age. In the Late Riphean, these morphotypes prevailed in many different-aged microbiotas. Moreover, in the middle and, particularly, upper parts of the Upper Riphean section, such microbiotas also contain several taxa. According to the general opinion, acanthomorphic (acanthaceous) acritarchs of the genera *Trachyhystrichosphaera*, *Prolatoforma*, *Cymatiosphaeroides*, and others are of particular biostratigraphic significance among such taxa.

Occurrence of genera *Palaeovaucheria* and *Majasphaeridium*, which are particularly typical of the Lakhandia microbiota, makes the second inference more preferable. It is noteworthy that similarity between microremains found in these sediments and Lakhandia fossils is evident from both the commonness of their taxonomic composition and the obvious similarity of preservation. Both microbiotas are dominated by large thick-walled forms with signs of bacterial and/or mineral destruction.

Paleoecological Interpretation of Sedimentation Settings for the Gray-Colored Sequence of the Molokovo Group

The microfossil assemblage established in siltstones and mudstones of the gray-colored sequence of Borehole North Molokovo is also found in other boreholes drilled in the Central Russian Aulacogen area (Danilovo-9, Bobrov, Roslyatino, and Velikii Ustyug). Although the taxonomic composition of the defined assemblages is less diverse, occurrence of some species similar to their counterparts from Borehole North Molokovo indicates the Late Riphean age of sequences in troughs of the East Mid-Russian segment.

Analysis of the taxonomic composition, sizes, and morphological features of microfossils allows us to make the paleoecological reconstruction of sedimentation settings. The examined samples contain a diverse acritarch assemblage with an anomalously high share of thin-walled forms with distinct signs of bacterial destruction, which are usually interpreted as remains of eukaryotic phytoplankton. Therefore, we can assume a relatively calm-water habitat of microorganisms in the basin and its difference from the Riphean epicontinental marine basins. Colonial coccoid microfossils typical of extended shallow shelf basins are entirely missing in the examined sediments, indicating isolation of the basin and contraction of the corresponding microbiota domain. This assumption is also confirmed by the insignificant share of filamentous forms, which are usually assigned to pro- or eukaryotic phytobenthic organisms. Thus, the specific composition of the microbiota in deepest sediments of

the Central Russian Aulacogen points to isolated character of sedimentary basins. This conclusion is consistent with the results of the facies analysis.

Geodynamic Formation Conditions and Composition of Rocks of the Molokovo Group

Comparison of the section of Borehole North Molokovo with sections of other boreholes drilled in the Central Russian Aulacogen area revealed their complete similarity.

The Molokovo Group is composed of feldspar—quartz and arkosic sandstones, feldspar—quartz siltstones, and chlorite—hydromica—mica—kaolinite mudstones with a variable silt admixture. The rock-forming clastogenic minerals are dominated by cataclased quartz derived from granite—gneiss rocks. Such rocks are developed in the basement of the Central Russian Aulacogen.

Thus, despite diverse sedimentation settings, the clastogenic framework of rocks in the section under consideration remained relatively constant: arkosic sandstone association remains unchanged in rocks through the entire Molokovo Group and indicates stable sources of detrital material. At the same time, one can suggest some maturation of material with time. Accumulation of the gray-colored sequence of the Molokovo Group reflects the first sedimentation cycle, i.e. destruction of basement rocks. Of particular importance was destruction of rocks in the “anomalous” part of the basement, such as mylonites and blastomylonites. Since the formation of the upper red-colored sequence of the Molokovo Group, the role of reworking (recycling) of sedimentary rocks became significant. This process is reflected well in the composition of rocks and primarily explained by the destruction of unstable sodium plagioclases during lithogenesis. Behavior of the $\text{Na}_2\text{O}/\text{K}_2\text{O}$ ratio in the rocks is remarkable: regardless of their type, this parameter exceeds 0.5 in the basement, is equal to 0.5 in the gray-colored sequence, and notably decreases upward the section beginning from the rocks of the red-colored sequence.

Comparison between compositions of the heavy fraction in sandy rocks of the gray-colored sequence in different boreholes demonstrates the occurrence of intervals enriched in clastogenic epidote. In some boreholes (for example, Roslyatino, Velikii Ustyug, and Bobrov), the epidote content in the heavy fraction amounts to 95–100%! The morphological similarity of clastogenic epidote grains in sandstones with metamorphic epidote developed after amphiboles and biotite in blastomylonites of the basement implies the existence of relationship between them. The comparative microprobe analysis of their chemical composition confirmed this assumption (Chamov et al., 2003).

Epidote is a characteristic mineral formed in the course of metasomatic transformations due to metamorphism. In terms of resistance to destruction, epi-

dote is attributed to the group of unstable minerals, which are rapidly destroyed both during redeposition and in the buried state. Occurrence of reactive solutions in the permeable sediments particularly stimulates the intralayer dissolution of epidote (Scheidegger et al., 1973; Chamov and Murdmaa, 1995).

These observations, combined with data on the roundness degree and fresh appearance of detrital material from rocks of the gray-colored sequence, suggest two important conclusions. First, metamorphic rocks of the basement served as a source of clastogenic epidote in sediments of the gray-colored sequence. Moreover, clastic material was not subjected to distant transport. Second, exhumation of tectonized rocks of the basement to the erosion zone was soon followed by accumulation of sediments. Therefore, weathering of detrital material and its significant chemical alteration was hampered.

It is remarkable that sections with epidote-rich intervals are unknown west of Borehole North Molokovo. For example, despite general similarity between sedimentary sections recovered by boreholes North Molokovo and Bologoe, drill core from the latter borehole lacks epidote.

DISTRIBUTION OF REFERENCE SECTION ELEMENTS ALONG THE STRIKE OF THE TRANSCRATONIC BELT

Direct Geological Observations

The position of the North Molokovo parametric borehole in the central part of the Central Russian Aulacogen allows us to trace the Precambrian rock complexes defined by drilling toward its northeastern and southwestern flanks.

Analysis of data provided by deep boreholes drilled along the strike of the aulacogen shows that sediments of the Molokovo Group, which reflect the entire development history of this structure, are distributed from the Kotlas—Yaren Trough to the Surazh, Vitebsk, and Mogilev troughs that are buried under sediments of the Orsha Depression. At the same time, completeness of the section and facies affinity of sediments vary along the strike of the aulacogen (Fig. 5).

For example, the northeastern flank of the aulacogen, which corresponds to the East Mid-Russian segment of the Transcratonic belt, is dominated by rocks of the gray-colored sequence of the Molokovo Group. Variegated sediments appear episodically among gray-colored minerals, for example, in sections of boreholes Roslyatino and Bobrov (Fig. 5). By their appearance and characteristic textural types, rocks from these intervals are identical to variegated sediments recovered by Borehole North Molokovo. According to the facies analysis, variegated and gray-colored sediments were accumulated in small lake-type basins and deep lakes, respectively. Thus, the structure of the sedimentary section at the northeastern flank of the aulacogen

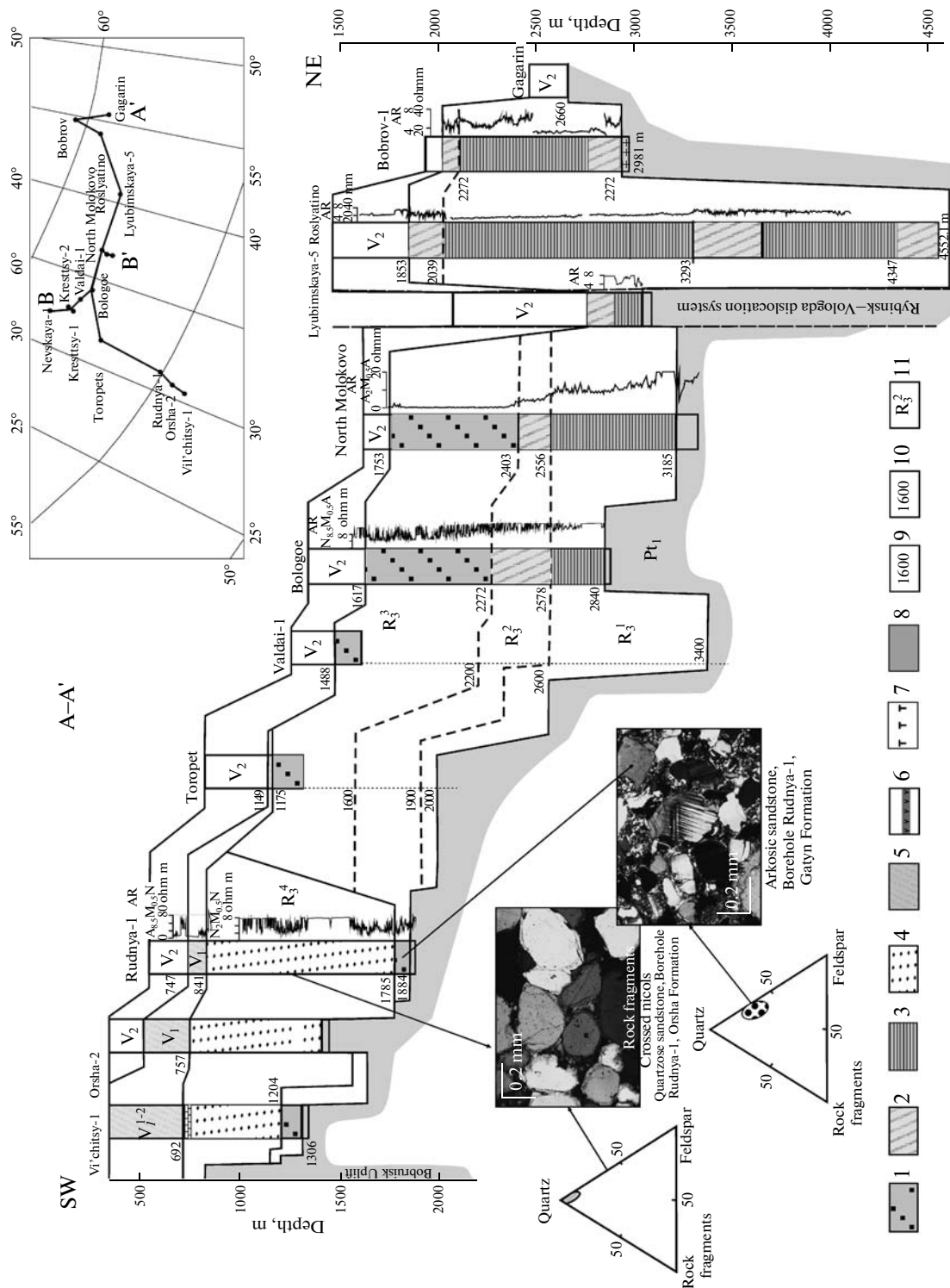


Fig. 5. Geological section (A—A') along the strike of the Central Russian Aulacogen. Positions of the profile and boreholes are shown in the inset. (1—4) Facies; (1) red-colored sandy sediments of intermontane troughs, (2) variegated sandy-silty-clayey sediments of shallow lakes, (3) gray-colored sandy-silty-clayey sediments of deep lakes, (4) red-colored sandy quartzose sediments of marine shoals; (5) volcanogenic-terrigeneous rocks; (6) dolerites; (7) tuffs; (8) basement; (9, 10) depth marks: (9) based on drilling data, (10) based on seismic data; (11) seismocomplexes: (R_1^1) mostly red-colored arkoses, (R_2^2) variegated arkoses, (R_3^3) red-colored arkoses, (R_4^4) largely quartzose red-colored sandstones, (V_1^{1-2}) undivided glacial, interglacial, and volcanosedimentary sequences, (V_2^2) volcanosedimentary sequences, (V_2) terrigenous and terrigenous-carbonate sediments. (AR) apparent resistivity.

cogen indicates intermittent shoaling of basins in this region, when conditions were favorable for a relatively compensated sedimentation. With respect to tectonics, section intervals with variegated sediments likely reflect stages of structural reorganization in the region. The structure of the Roslyatino Trough section suggests three stages of such reorganizations, and the first stage was marked by initiation of the basin proper. The distribution area of the gray-colored sediments indicates that no significant lateral expansion of sedimentary basins occurred at that time. Tectonic subsidence remained a leading factor responsible for the formation of the accommodation space.

In the central part of the aulacogen, sedimentation was characterized by the an irreversible trend with transition from the deep lacustrine gray-colored to the distinctly subaerial red-colored sediments. The development area of red-colored and variegated sediments substantially exceeded that of their gray-colored counterparts. In many areas of the southwestern aulacogen, red-colored sediments advanced from individual troughs to form a single field. This implies a progressive tectonic evolution, when expansion of the strike-slip fault zone was accompanied by lateral migration of sedimentary basins up to the point of their junction and formation of small synclinal structures. Shoaling of sedimentary basins, which was particularly distinct in the southwestern direction, stimulated development of conditions favorable for compensated deposition.

The general and regular uplift of basement in the southwestern direction resulted in the disappearance of basal elements (gray-colored and variegated sequences) from the sedimentary cover section. They are missing in sections west of the Velizh Saddle, and only thin sediments of the red-colored sequence are observed in the Belarus territory.

We believe that degeneration of structures of the Central Russian Aulacogen in Belarus is caused by its tectonic development as a complex strike-slip fault structure (Chamov et al., 2001, 2003; Kostyleva et al., 2001; Chamov, 2004, 2005). In our opinion, the development history of the aulacogen culminates in the formation of the red-colored sequence, while overlying elements of the Precambrian sedimentary cover were forming under a platformal tectonic regime. Indeed, sediments of the Molokovo Group over the major portion of its distribution area are blanketed by shallow marine facies of the Upper Vendian Valdai Group. These sediments, which are readily recognized in the section based on lithofacies and petrophysical criteria (for example, high-resistance horizon inside the Redkino sediments), mark initiation of the Moscow Syncline, i.e., transition from the platformal to the plate development stage.

A different situation is observed in the Orsha Depression superimposed on the degenerated structures and pinchout of sedimentary complexes of the Central Russian Aulacogen (Figs. 1 and 5). The red-

colored sedimentary rocks in the depression are attributed to the Belarus Group scrutinized in (Makhnach et al., 1975, 1976; *Geologiya...*, 2001; Nagornyi, 1990; and others). They substantially differ from the underlying red-colored sediments of the aulacogen in several parameters. Among them, the dominant quartz composition, high mineralogical maturity, and clinoform position of these sediments are most important (the latter property readily recognized in CMP records is discussed below).

The study of thin sections kindly donated by N.V. Veretennikov offered an opportunity for the comparison of their composition with that of sandstones from the Central Russian Aulacogen. The drastic replacement of arkosic sandstones of the red-colored sequence of the Molokovo Group by their highly mature counterparts from the Belarus Group is particularly distinct in the section of Borehole Rudnya-1 (Fig. 5). It is clear that rocks of the Molokovo and Belarus groups were deposited in different sedimentation settings and they received detrital material from different sources. The last assumption is confirmed by the special study of quartz grains conducted in line with the technique described in (Simanovich, 1974). For example, it was established that detrital quartz in sandstones of the Belarus Group is largely characterized by hydrothermal and intrusive genesis. In arkoses of the Molokovo Group, the quartz is derived from the eroded granite-gneiss rocks (Kostyleva and Simanovich, 2007).

Thus, sediments of the Molokovo Group in the aulacogen are overlain in their entire distribution area by rocks of the Valdai and Belarus groups that were formed in different lithogeodynamic settings. Occurrence of quartz sandstones in the section of the Orsha Depression suggests the following conclusion: Transition from the aulacogen to the plate stage in the platform development occurred during a relatively short geological period; this process was accompanied by the formation of specific conditions favorable for the accumulation of a thick and highly mature quartz sequence in a limited area. The development of its formation model is a task for future studies.

We studied the tectonic mélange series in sections of many deep boreholes drilled in the Central and East Mid-Russian segments. As is shown below, directive textures typical of rocks from this series are related to dynamometamorphism and cataclasis. In CMP records, they demonstrate distinct "stratification" similar to that in sedimentary sections. Therefore, it is difficult to carry out an exact discrimination between the sedimentary cover and basement, but we can affirm that tectonized rocks of this series are developed over the entire Central Russian Aulacogen.

The isotopic studies reveal rejuvenation of these rocks from the northeast to southwest. This is also evident from the data on accessory zircons from tectonized granodiorites of the basement penetrated by Borehole Nevskaya-184. The results of these studies are

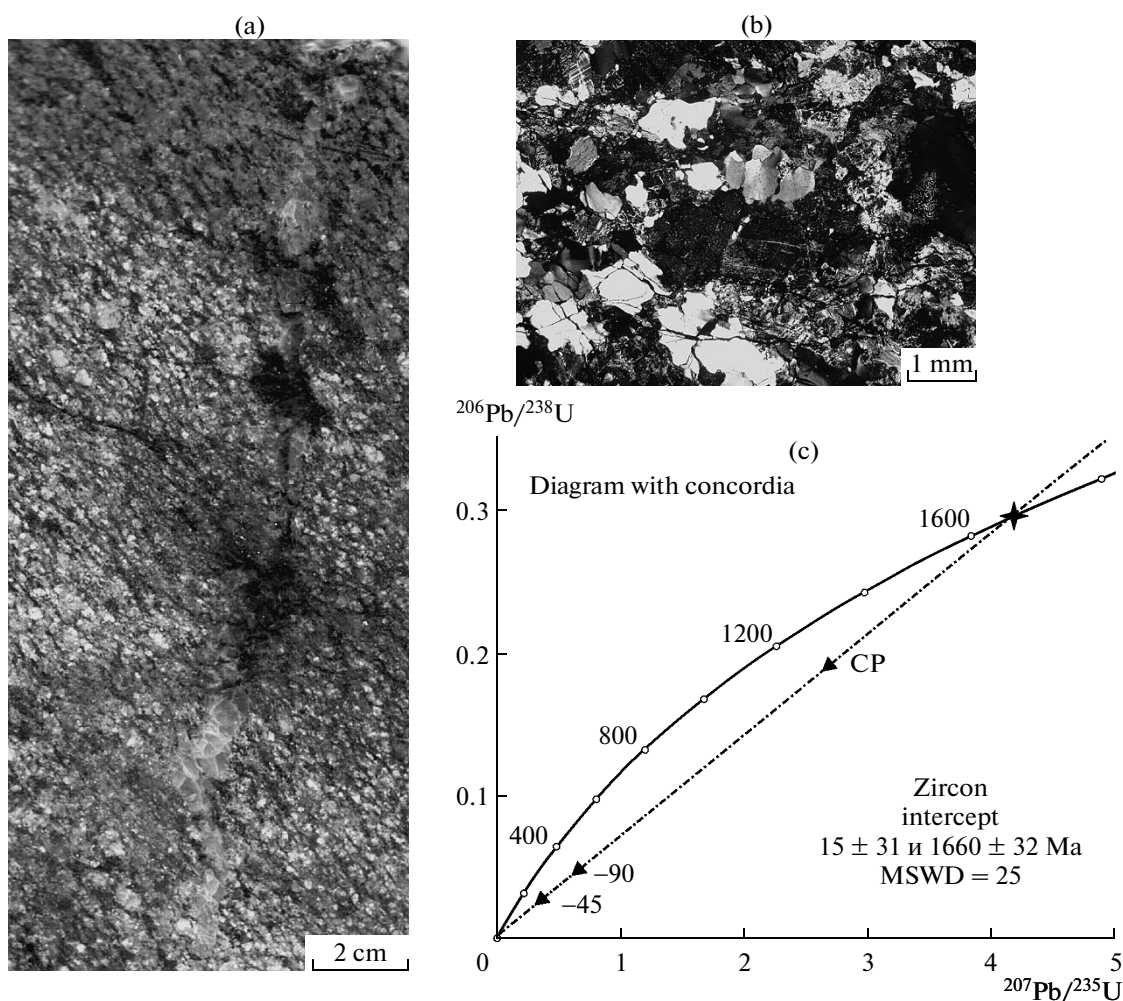


Fig. 6. Results of the mineralogical-petrographic and U-Pb isotopic studies of mylonitized granodiorites from Borehole Nevskaya-184. (a) Chip section; (b) thin section, crossed nicols; (c) isochron based on the results of isotopic studies.

shown in the table and the diagram with concordia (Fig. 6). The uranium contents in zircons, particularly in the fine-grained ($<45 \mu\text{m}$) fraction, exceeds 2000 ppm, resulting in high discordance of ages. Zircon was almost completely dissolved during the acid treatment. Nevertheless, the residue left after this procedure also remained discordant. All this provokes significant errors in the calculated discordia age (estimated at $1660 \pm 32 \text{ Ma}$) and high MSWD. The lower discordia intercept is located near zero, which points to recent Pb losses by the metamictic zircon.

Correlation between Direct Geological Observations and Seismic Prospecting Data: Characteristics and Distribution of Seismocomplexes

The characterized sequences defined in borehole sections based on direct geological studies are characterized by specific seismic wave patterns. Therefore, such sequences are readily recognized in the CMP records.

For example, the fragment of time section 029302, which crosses the Molokovo basin of the Valdai-Molokovo Trough in the meridional direction, clearly demonstrates systems of reflecting surfaces (Fig. 7). They differ in both patterns and intensity of the wave field because of specific lithological features of rocks and their bedding types. The assumption that precisely sequences of the Molokovo Group represent elements of the sedimentary section is confirmed by the coincidence of seismic reflectors and geological boundaries established by drilling. This is clearly demonstrated by spontaneous polarization and neutron gamma logs: intensity jumps in logs correspond to interfaces between seismic complexes (Fig. 7). This regularity is observed both in the central part of the basin (Borehole North Molokovo) and on its southern slope complicated by normal faults (Borehole R-3).

Analysis of the time section provides grounds for defining and tracing across the strike of the Molokovo basin five seismocomplexes corresponding to the Precambrian part of the sedimentary section and upper

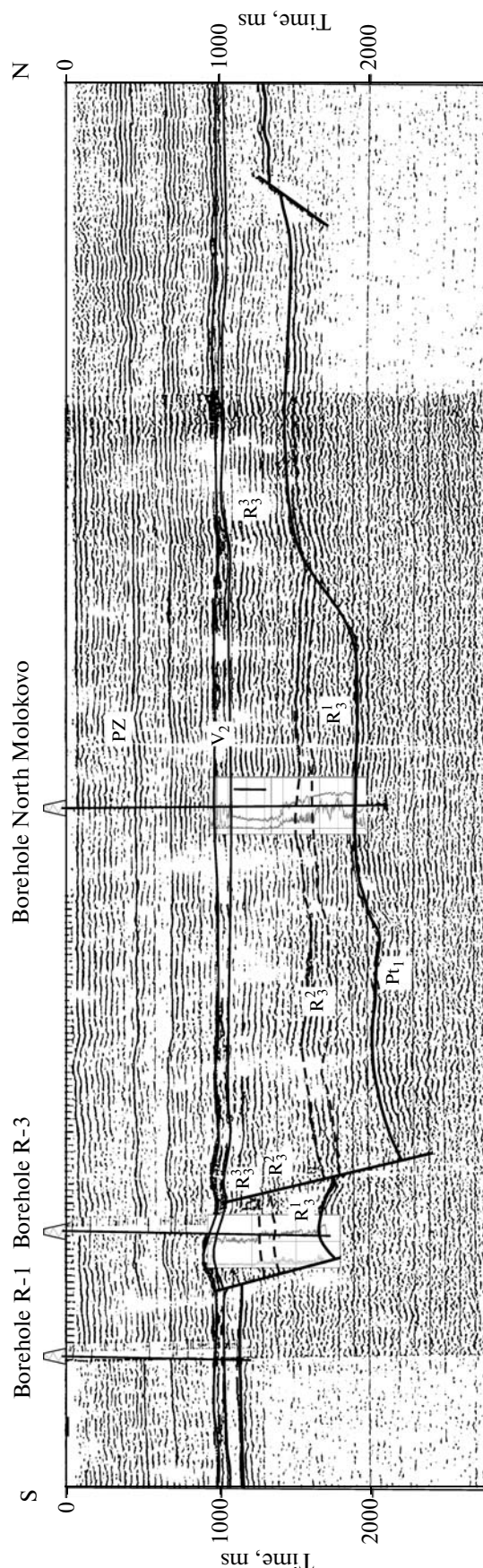


Fig. 7. Sequences of the Molokovo Group and tectonic mélange in the fragment of time section 029302. For boreholes R-1 and North Molokovo, spontaneous polarization and neutron gamma logs are shown.

part of the basement (from the top to bottom): Upper Vendian (V_2) plate complex; Upper Riphean (R_3^3 , R_3^2 , and R_3^1) preplate complexes corresponding to the red-colored, variegated, and gray-colored sequences of the Molokovo Group; and Lower Proterozoic (Pr_1) tectonic mélange complex.

In the similar manner, based on the analysis of CMP records and deep drilling data, we carried out seismostratigraphic subdivision of the Precambrian sedimentary section and upper part of the basement in the Central Russian Aulacogen and Orsha Depression.

The Upper Riphean–Vendian part of the sedimentary cover comprises eight seismocomplexes, combination of which depends on the particular structure. The Central Russian Aulacogen includes the following seismocomplexes: (R_3^1) mostly gray-colored arkoses; (R_3^2) variegated arkoses; (R_3^3) red-colored arkoses; and (V_1^2) volcanogenic–terrigenous sediments. The Orsha Depression section includes the following complexes: (R_3^4) red-colored (largely quartzose) sandstones; (V_1^1) glacial and interglacial sediments; and (V_1^2) variegated volcanogenic–terrigenous sediments. The upper seismocomplex (V_2) is represented by terrigenous and terrigenous–carbonate rocks. It corresponds to the basal part of the Moscow Syncline and overlies Riphean–Lower Vendian sedimentary complexes of the Central Russian Aulacogen and most part of the Orsha Depression. A single seismocomplex (Pr_1) represented by dynamometamorphosed rocks is defined in the upper part of the basement.

Figure 8 demonstrates characteristic wave patterns of these seismocomplexes, their distribution along the strike of the Transcratonic belt structures, and relationships with the previously defined stratigraphic units (groups and formations). As follows from the figure, the defined seismostratigraphic units of the section are inconsistent with stratigraphic units accepted by the Interregional Stratigraphic Commission.

No special explanations are needed for the most part of the Central Russian Aulacogen: seismocomplexes reliably defined based on the wave patterns naturally include numerous stratigraphic units outlined by rhythmostratigraphic data. It is clear that, at least for the Central Mid-Russian segment, ages of local stratigraphic units should be revised with account for the data on microphytological remains from the fine-grained sediments in the lower part of the gray-colored section of Borehole North Molokovo, where the rep-

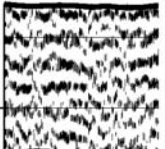
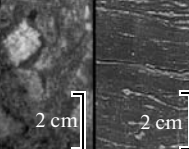
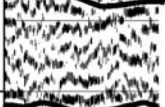

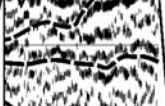

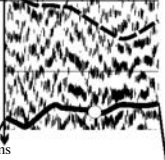
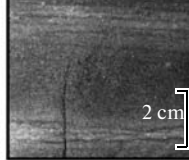
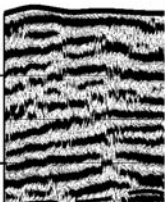
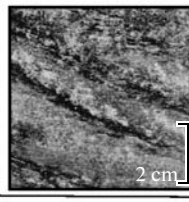


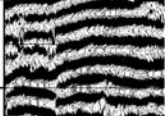
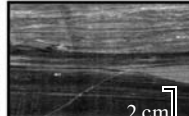
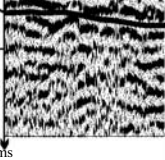



General stratigraphic chart				Structural level	Geotectonic stage	Group	Seismocomplex	Lithology		
Erathem	System	Subsystem	Ma					In-dex	Fragments of timesections	Type rock samples
Upper Riphean	Vendian	Upper	850	sedimentary cover	syncline	Valda	V ₂			Brecciaconglomerate, unsorted with sandy matrix. Sandstones (gray, inequigranular, medium- to fine-grained, oligomictic feldspar—quartzose) and siltstones (clayey, calcareous). Mudstones (dark gray, silty, chlorite—mica—kaolinite). Bedding: horizontal, wavy, lenticular, frequently disturbed by underwater slump processes. Facies: shallow-water and coastal-marine sediments (Makhnach et al., 2001).
						Volyn	V ₂ ¹			Sandstones, siltstones, and clays (red-brown to greenish gray in some places). Detrital material: with admixture of decomposed pyroclastics and fragments of volcanics. Bedding: horizontal, lenticular. Facies: shallow-marine (Makhnach et al., 2001)
		Vil'chany				V ₁ ¹			Red-brown (locally light gray) sandy—silty—clayey rocks with inclusions of coarse-detrital material. Bedding: horizontal, ribbon-like. Facies: glacial and interglacial sediments(Makhnach et al., 2001).	
	protosyncline	Belarus			R ₃ ⁴			Sandstones (pinkish, light brown-red, quartzose or feldspar—quartz, micaceous—kaolinite, moderate- to well-sorted). Detrital material sub- and well-rounded. Bedding: horizontal, cross, cross-wavy. Facies: shallow-water and coastal-marine sediments.		
		aulacogen			Molokovo	R ₃ ³			Sandstones (red-brown and lilac-brown, arkosic, oligomictic feldspar—quartz, fine- to medium-grained, frequently with gravel admixture, poorly sorted). Detrital material moderately rounded. Rocks (incoherent, massive or weakly cemented, with large-scale unidirectional cross- and cross-wavy bedding). Facies: sediments of intermontane depressions.	
						R ₃ ²			Alternating brown and gray medium- to fine-grained sandstones, clayey siltstones, and silty mudstones. Bedding: small-scale wavy, cross-wavy, cross. Sandstones (arkosic and oligomictic feldspar—quartz) Detrital material moderately sorted, angular to subrounded. Facies: sediments of shallow lakes.	
R ₃ ¹				Alternating gray silty mudstones, feldspar—quartz siltstones, and fine-grained sandstones. Bedding: horizontal, small-scale wavy, lenticular, cross-wavy. Slickensides with inclination up to 45°. Sandstone (inequigranular, fine- to medium-grained, poorly sorted, oligomictic and arkosic feldspar—quartz). Facies: sediments of deep lakes.						
Upper Karelian			1650	basement		Tectonic mélange	Pt ₁ ¹			Dynamometamorphosed rocks of the epidote—amphibole facies. Fragments of pinkish migmatized granitoid rocks in gray blastomylonitic matrix with distinct directive textures.
			1800							

Fig. 8. Seismogeological complexes of the Central Russian Aulacogen and Orsha Depression and their relationships with stratigraphic units accepted by the Interregional Stratigraphic Commission.

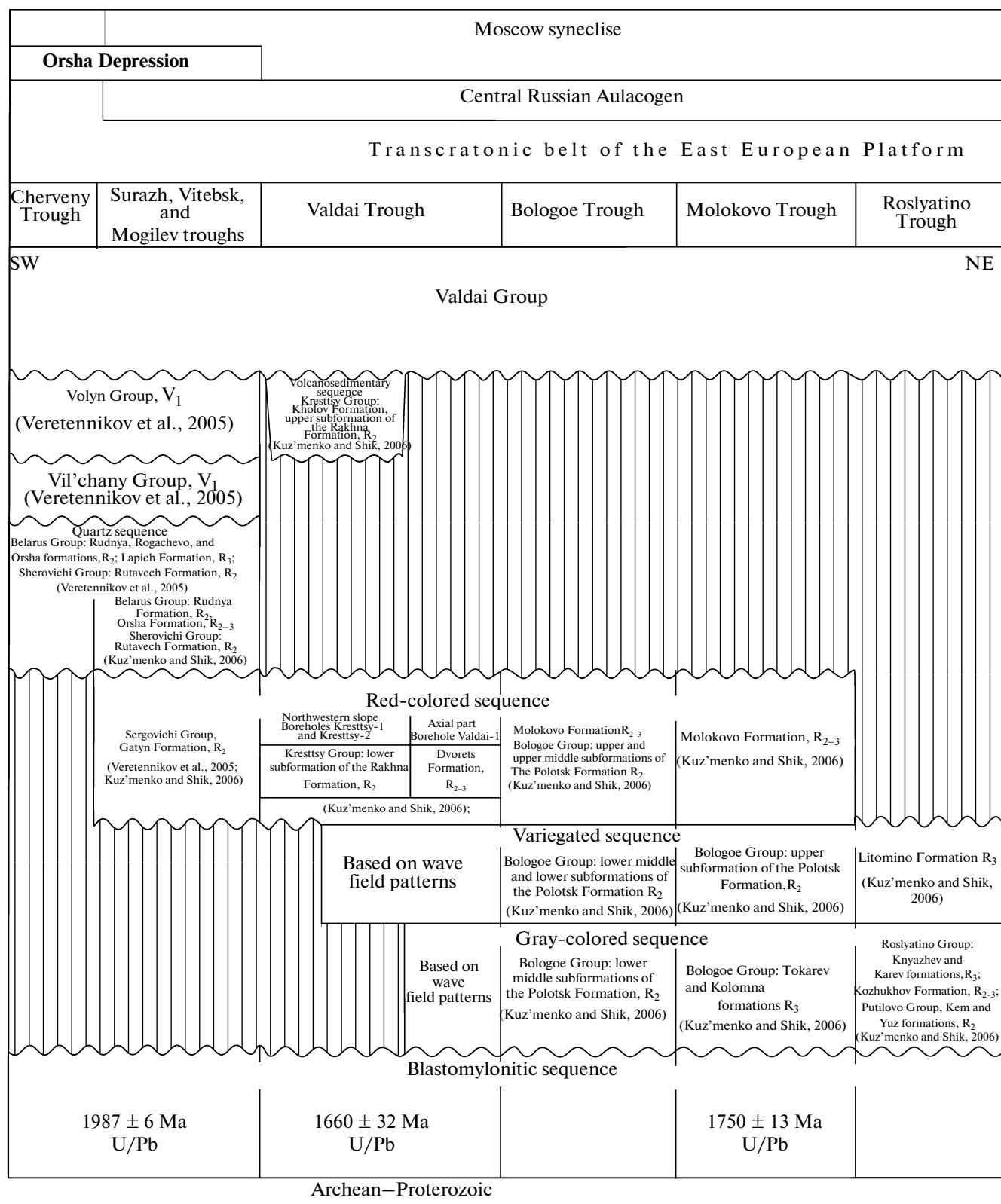


Fig. 8. Contd.

Fig. 9. Sections of the Valdai–Molokovo Trough along profile B–B': (a) Geological section according to drilling data; (b) seismogeological section based on a fragment of time section 090070. See Fig. 5 for positions of profiles and legend.

representative assemblage of microfossils indicates the absence of pre-Upper Riphean sediments (Fig. 4).

Main contradictions between seismocomplexes and stratigraphic units are revealed during the study of transboundary structures of Russia and Belarus. This statement is primarily valid for volcanosedimentary complexes developed at the flank of the Valdai–Molokovo Trough and quartz sequences of the Orsha Depression. The essential explanations are given below in the descriptions of seismocomplexes.

Seismocomplex Pr_1 characterizes the upper part of the basement and corresponds to rocks of the tectonic *mélange* series.

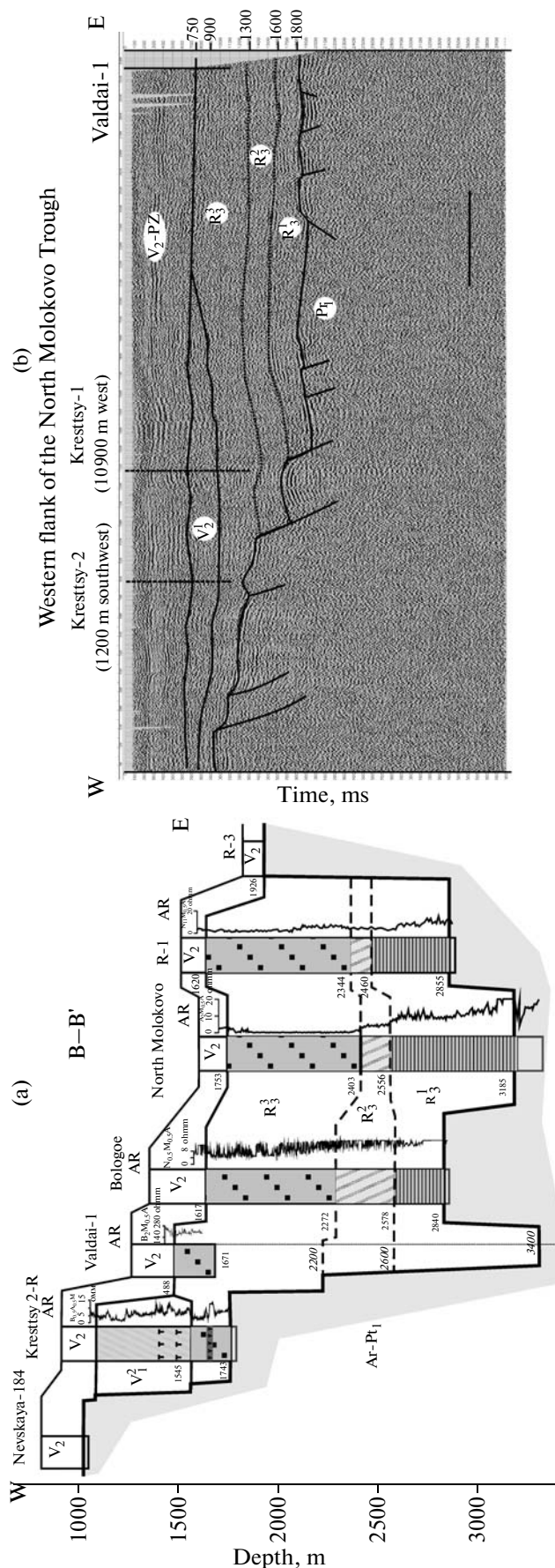
Wave patterns of the seismic record are variable along the aulacogen strike, and the seismocomplex is represented by both chaotically located discontinuous reflection surfaces and systems of parallel subhorizontal reflectors.

In some areas, significant segments of seismic records demonstrate that the boundary between sedimentary and crystalline rocks is masked by the development of seismically stratified sequences of unclear genesis and age. This phenomenon is observed over the entire Central Russian Aulacogen and beneath sedimentary complexes of the Orsha Depression. Based on intensity of reflections and stratification patterns, such sequences are usually attributed to the sedimentary cover. At the same time, they represent tectonically laminated basement rocks in some places.

Fragments of seismic records of the wave field obtained in the Molokovo basin clearly exhibit that the sedimentary cover is underlain by subhorizontal and inclined packets of parallel reflectors in the wave field of the basement (Figs. 2, 7). In these areas, the stratal velocity of seismic waves between the basement top and depths of approximately 350 m below the basement does not exceed 5.3 km/s, while the velocity increases to 6.0–6.2 km/s below this depth. Density of rocks in core varies from 2.5 to 3.15 g/cm³ (average 2.77 g/cm³).

As was shown by drilling of the North Molokovo parametric borehole, the low-velocity part of the basement is composed of blastomylonites, which form a tectonic *mélange* representing a foliated matrix with submerged granodiorite blocks.

Stratification of the basement is traced in seismic time sections along the strike of troughs constituting the Central Russian Aulacogen in the western direction up to the Baltic Shield. Thickness of stratified members amounts to 300 m or more. Of particular interest are profiles 090070 and 090005 with closely located boreholes, which penetrated the basement at



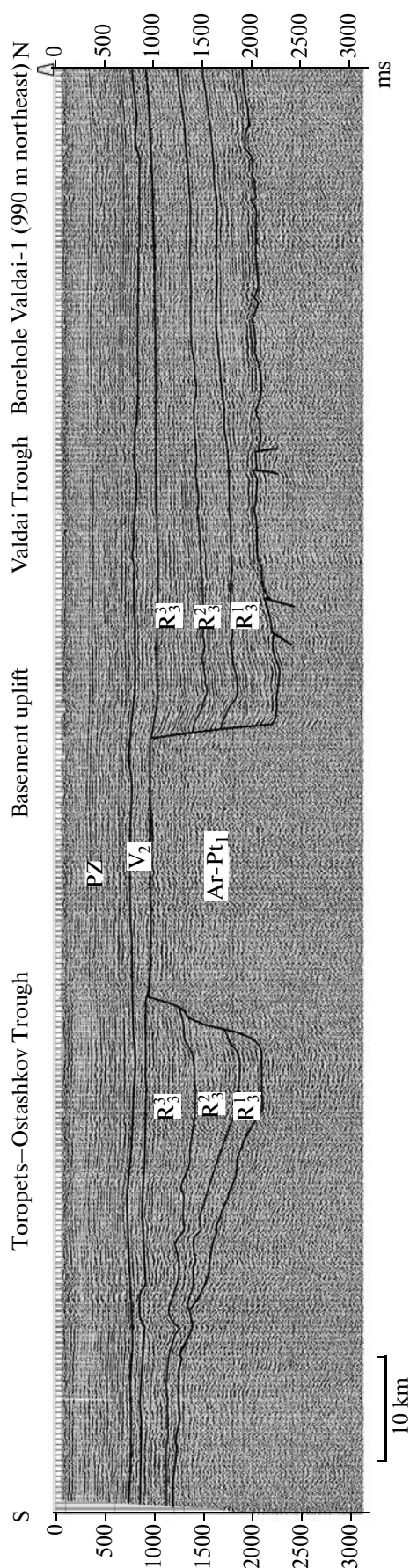


Fig. 10. Seismogeological section across the strike of the Valdai–Molokovo and Toropets–Ostashkov troughs (fragment of time section 090002). See Fig. 1 for position of the profile.

depths corresponding to stratified seismic members: Borehole Kresttsy-2 located 1200 m southwest of Profile 090070 recovered the basement rocks at a depth of approximately 1750 m; Borehole Bologoe-1 located 700 m west of Profile 090005 reached the basement at a depth of 2850 m. The record obtained along Profile 099970 clearly demonstrates that stratified areas are isolated from each other corresponding to different blocks and appear to be located at different hypsometric levels at the transition between flanks of the trough and slope of the Baltic Shield (Fig. 9).

If drilling data are unavailable, the nature of stratified series at the sedimentary cover/basement boundary remains unclear. For example, the base of seismocomplex R_3^1 at the southwestern flank of the Valdai Trough is marked in the record by a seismic member with intense continuous and distinctly stratified reflectors. In the time section, this member is characterized by the sustained thickness and the number of reflections (phases) within the member remains constant. Judging from these features, the member should be attributed to the sedimentary cover. Since this seismic member is bounded by faults along the strike of the trough, one can assume that the member characterizes sediments of the early (pre-aulacogen?) graben or the most subsided (therefore, more compact) part of the aulacogen. At the same time, only this member exhibits displacements of the reflection packet typical of block movements in the basement.

The exact position of the lower boundary of sedimentary cover is essential for the determination of its range, which, in turn, is important for the assessment of its economical potential. In December 2008, at the meeting of representatives of the Department of Geology (Ministry of Natural Resources and Environment Protection, Belarus Republic), Belgeologiya Regional Agency, Institute of Nature Management (National Academy of Sciences, Belarus Republic), Geological Institute (Russian Academy of Sciences), and VNII-Geofizika Federal State Unitary Enterprise dedicated to the geological study of transboundary areas in the framework of solutions of 9th–11th sessions of the Intergovernmental Council of CIS countries, issue of the genesis and age of new seismically stratified sequences at the basement/sedimentary cover boundary was put forward as a first-priority task.

Seismocomplex R_3^1 corresponds to the gray-colored sequence of the Molokovo Group. In terms of the specified stratigraphic scheme (Kuz'menko and Shik, 2006), this seismocomplex comprises the Tokarevo and Kolomna formations, middle and lower subformations of the Polotsk Formation (Bologoe Group)

and, presumably, formations of the Roslyatino and Putilovo groups (Fig. 8).

Wave pattern within this seismocomplex varies along the aulacogen strike, but distinctly extended reflectors prevail. In some places near trough slopes, the pattern becomes complicated and the seismic record demonstrates clinoform bodies.

The seismocomplex is reliably traced over the most part of the Central Mid-Russian segment. As compared with the overlying seismocomplexes of the Molokovo Group, this complex is characterized by a smaller distribution area. This regularity is expressed well in different troughs of the aulacogen (Figs. 7, 9, and 10).

The seismocomplex disappears completely from the sedimentary cover section southwest of the Toropets basement uplift. The available seismic materials provide no opportunity for tracing the seismocomplex in the East Mid-Russian segment. At the same time, similar petrophysical properties of rocks from the gray-colored sequence drilled by boreholes suggests that seismocomplex R_3^1 likely constitutes the main part of the preplate sedimentary cover at the northeastern flank of the aulacogen.

Seismocomplex R_3^2 corresponds to the variegated sequence of the Molokovo Group. According to the specified stratigraphic scheme (Kuz'menko and Shik, 2006), this complex characterizes the lower subformation and basal middle subformation of the Polotsk Formation (Bologoe Group) and Litomino Formation (Roslyatino Group) (Fig. 8).

This seismological complex is characterized by various reflections in different parts of the section, probably due to the heterogeneity of its lithofacies composition. For example, intense curved (frequently discontinuous) reflectors are recorded in the northeastern part of the aulacogen, whereas the southwestern is dominated by distinct intense reflectors traced over a significant distance.

The seismocomplex crowns the Upper Riphean section in troughs of the East Mid-Russian segment and is universally developed over the Central Mid-Russian segment. Thickness of the complex is relatively stable (450–600 m) in the northeastern part of the segment, but it complete pinches out south of the Toropets Uplift.

Along the strike of the aulacogen, seismocomplex R_3^2 occupies different structural positions relative to basement uplifts. Along Profile 090002, the seismocomplex is truncated by the basement uplift that separates the Valdai–Molokovo and Toropets–Ostashkov troughs (Fig. 10). At the same time, the complex overlies the southwestern continuation of this uplift near Belarus and unites structures of these troughs into a single sedimentary basin. Thus, seismocomplex R_3^2 occupies a wider area than the lower seismocomplex

due, in particular, to its greater expansion in the southwestern direction.

Seismocomplex R_3^3 corresponds to the variegated sequence of the Molokovo Group. The seismocomplex correlates with the Molokovo Formation, upper subformation and upper middle subformation of the Bologoe Group, and lower subformation of the Rakhna Formation in the stratigraphic scheme (Kuz'menko and Shik, 2006) specified for the Central Russian Aulacogen. This complex matches the Gatyn Formation (Sherovichi Group) in the sedimentary section of the Orsha Depression (Veretennikov et al., 2005; Kuz'menko and Shik, 2006) (Fig. 8).

In the wave field, the seismocomplex is characterized by distinct intense (frequently discontinuous) reflectors and subhorizontal extended reflection packets. Boundary with the overlying Upper Vendian sediments is readily recognized owing, in particular, to distinct curved reflection packets pinching out under the Upper Vendian seismocomplex.

In the Central Mid-Russian segment, the seismocomplex under consideration is characterized by the widest distribution. It significantly overlies the older seismocomplexes R_3^1 and R_3^2 (Figs. 7, 9, and 10).

In the southwestern direction, thickness of the seismocomplex decreases from 1000 to 250 m. Similar to the underlying seismocomplexes, its distribution is limited by aulacogen branches in the central and northeastern parts of the segment, although it is also typical of a relatively spacious sedimentary basin at the southwestern flank.

South of the Velizh Saddle, the given seismocomplex is truncated by the overlying seismocomplex R_3^4 and recognized in separate negative structures of the basement.

Seismocomplex R_3^4 is universally developed in the superimposed structure of the Orsha Depression. Here, the seismocomplex characterizes the Rutavech Formation (Sherovichi Group) and the Rogachevo, Rudnya, Orsha, and Lapichi formations (Belarus Group) (Fig. 8).

The keyboard-type block surface of the crystalline basement and the red-colored sediments of the aulacogen preserved in buried structures (Seismocomplex R_3^3) serve as a lower boundary for this seismocomplex. The complex is bounded from above by Lower Vendian sediments (Seismocomplex V_1^{1-2}). The surface of the latter complex is very uneven with a height difference of (at least of 250 m). Thickness of the seismocomplex rapidly (but gradually) decreases from 600 m in the southwest to 0 m in the northeast, where it pinches out under the Vendian seismocomplex north of Velizh.

Time section along the Cherikov–Orsha–Usvyaty profile carried out by Belarussian geologists

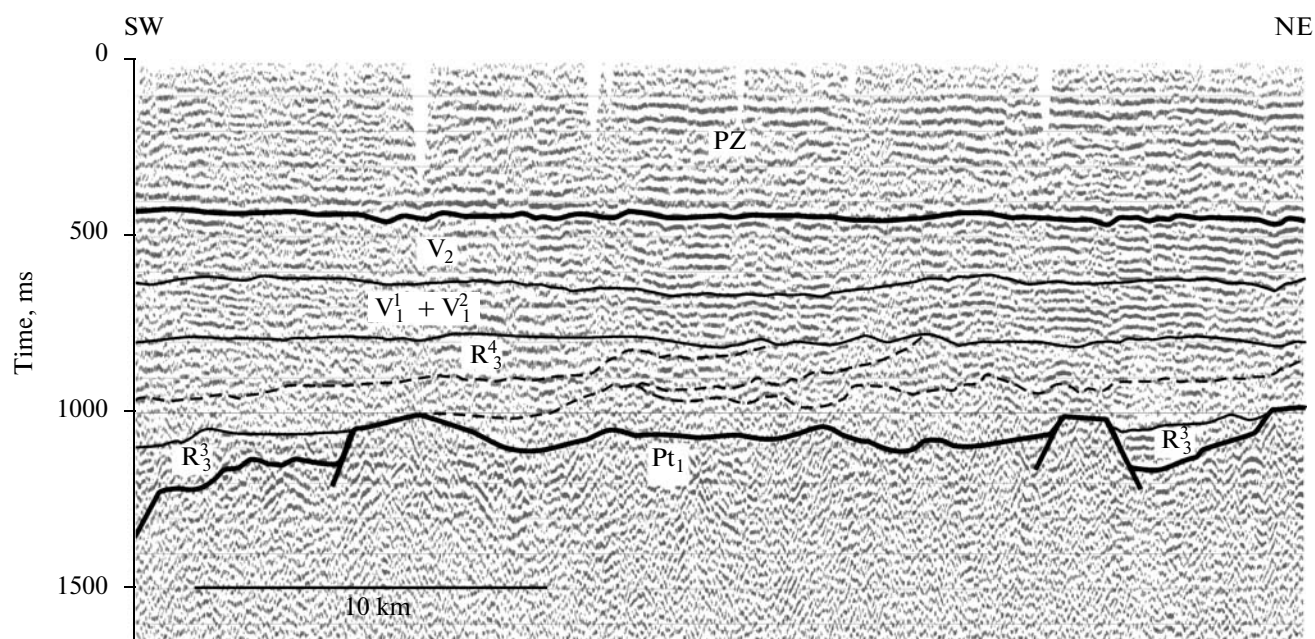


Fig. 11. Relationship between R_3^4 (quartz sands of the Belarus Group) and R_3^3 (red-colored arkoses of the Molokovo Group) seismocomplexes. A fragment of time section along the profile from Velizh to the state boundary line. See Fig. 1 for position of the profile.

(Razlomy..., 2007) and reinterpreted on the initiative of Yu.A. Volozh (GIN RAN) clearly demonstrates a bean-shaped structure of the sesimogeological complex. The complex is characterized by gentle southward inclination and intense discontinuous (distinctly stratified in some places) seismic reflections.

A similar situation is also observed in the Russian territory crossed by the Toropets–Velizh–state boundary profile. Fragments of the time section shows a cliniform occurrence of the Orsha seismocomplex R_3^4 on relicts of sesimocomplex R_3^3 localized in graben structures (Fig. 11). Such a structure is explained by the development of progradation lobes, the orientation of which indicates the transport of clastic material in the southern and southwestern directions.

The observed relationship between seismocomplexes suggests the following points: (1) formation of seismogeological complex R_3^4 as a single body with the progradation structure; (2) development of a compositionally specific erosion area northeast of the present-day position of the complex; and (3) regressive character of sedimentation, when compensated sedimentation took place in a newly formed structural trap.

Seismocomplex V_1^1 corresponds to glacial and interglacial sediments referred to the Lower Vendian Vil'chany Group (Veretennikov et al., 2005). The seismocomplex is characterized by a chaotic pattern of the

wave field. This feature, combined with the insignificant thickness and irregular lateral distribution of the seismocomplex, hampers its reliable recognition in the seismic record. The seismocomplex is readily recognized only in the Orsha Depression in the southwestern part of the study region.

Seismocomplex V_1^2 corresponds to volcanosedimentary rocks of the Volyn Group in the Orsha Depression and the upper subformation of the Rakhna Formation and Kholov Formation (Kresttsy Group) at the northwestern flank of the Valdai–Molokovo Trough (Fig. 8).

We believe that this seismocomplex also includes gabbro–dolerite stratiform bodies intruding the underlying red-colored sequence R_3^3 . Precisely these igneous and sedimentary rocks likely correlate with volcanosedimentary sequences of the Volyn Group (Orsha Depression) and Lower Vendian sills and basalts (Volyn Trough).

The structure and position of seismocomplex V_1^2 on the slope of the Valdai Trough deserve special attention. The seismocomplex under consideration characterizes a volcanosedimentary sequence, which has no analogues in Riphean sections of the Valdai–Molokovo or other troughs of the Central Russian Aulacogen. Nevertheless, despite the exotic features of these sediments, they provided ground for many theoretical constructions, which provoked a significant confusion

in understanding the structure and development history of this complex region.

The Kresttsy boreholes recovered a section atypical of the southwestern Moscow Syncline, where the interval of 1545–1185 m corresponds to the volcanosedimentary sequence. In the 1960s, K–Ar datings (Geisler, 1966) of bulk samples of volcanogenic rocks yielded ages ranging from 1245 to 1353 Ma for the lower subformation (dolerites, depth approximately 1630 m) and about 1180 Ma for the upper formation (volcanic tuff, depth 1470 m). At present, these ages cannot be considered, however, as reliable one. Therefore, A.A. Klevtsova and, subsequently, Yu.T. Kuz'menko and S.M. Shik justly attributed this sequence to the higher stratigraphic level (Rakhna Formation, upper subformation; Kholov Formation).

The structural position of this sequence in the preplate cover section was not checked by seismic methods. We correlated sections of the preplate cover recovered by boreholes in the Valdai–Molokovo Trough. Borehole columns correlate with the corresponding hypsometric levels in the geological section. This fact emphasizes the stepped structure of the basement surface (Fig. 9a). The stepped character of the profile resembles a similar regular westward uplift of the basement established for the entire Central Russian Aulacogen (Fig. 5). It is well seen that gray-colored and variegated sediments disappear in the section when approaching the western flank of the profile (fault-related steps of the Valdai Trough slope) due to structural and facies variations near the slope of the trough. As was shown above, these sediments, which are missing at the flanks, appear again as a thick sequence along the southwestern Valdai–Demyansk–Nakhod–Toropets–Velizh profile. This observation is also confirmed by the distribution pattern of the defined seismocomplexes with gradual disappearance of the lower elements from the preplate section (Fig. 9b).

Seismogeological complex V_1^2 occupies the highest hypsometric position above the Upper Riphean seismocomplexes R_3^1 – R_3^3 that are reliably traced along the Valdai–Molokovo Trough. In other words, the sediments characterized by this seismocomplex have no relation with the basal part of the Precambrian sedimentary section and cannot be older than the Late Riphean. Analysis of the wave field pattern obtained for the section indicates that seismocomplex V_1^2 occurs in the sedimentary cover as a lens sandwiched between the Upper Riphean preplate and Upper Riphean plate seismogeological complexes (Fig. 9b).

Taking the structural position of the volcanosedimentary sequence and lack of volcanic products in Upper Riphean sedimentary rocks into consideration, the given seismogeological complex should be attributed to the Lower Vendian. Local manifestations of volcanism and intrusion of the stratiform body into the

underlying Riphean sequences are recorded in the tectonically most mobile area (slope of the Valdai Trough). These processes could be provoked by structural reorganization of the region after termination of the aulacogen development.

CONCLUSIONS

The main results of this study are as follows.

Regularities in the structure of the Precambrian sedimentary section and upper part of the basement were analyzed. Boundaries of the cover and basement were specified, and an additional trough was defined. These observations expand the sedimentary part of the section and enhance economical potential of the study region.

The Precambrian section recovered by Borehole North Molokovo is proposed as a reference one for the Central Russian Aulacogen.

Seismocomplexes defined in the wave field of CMP seismic records allow us to trace rock members and sequences established by drilling in troughs of the aulacogen. The seismocomplexes correlate with stratigraphic units in available local scales.

Discordance between the proposed seismostratigraphic elements of the section and local stratigraphic units seems to be unavoidable during the revision of methodological approach to correlation between elements of the Precambrian section.

Notions on the composition of sedimentary complexes and their stratigraphic organization used as a basis for the available stratigraphic schemes were analyzed from the “top to bottom,” i.e., in the theoretical framework of the platform cover development. Correlation of sedimentary section both within individual structures and between them was conducted with account for the plate stage in platform development, i.e., based on the concepts of existence of spacious subsidence areas (synclises) against the background of a calm (platform proper) tectonic regime. Methods of the lithofacies and rhythmostratigraphic analysis with account for standard logging materials was and remains as the main methodological approach to subdivision of the sedimentary section and correlation of stratigraphic units defined in individual boreholes. Efforts of geologists engaged in such analysis are aimed at tracing rock formations through the entire or most part of the platform.

Such an approach, however, ignores the complex structural organization of troughs of the Central Russian Aulacogen, which are filled by sediments of the preplate stage. As was shown above, these troughs represent spatially isolated pull-apart structures located at different hypsometric levels (Figs. 1, 5). Despite the similarity of sedimentary processes, each of these basins represented an individual sedimentological trap with unique facies of sediments. The shear nature of these pull-apart basins—changes in geometry during

their growth, transport of detrital material largely along transform depressions, and sedimentological isolation—was responsible for rapid facies variations even within individual structures. For example, fault-line and near-slope facies sharply differ from their counterparts in central parts of the basin (Chamov et al., 2003).

The sediments of neighboring basins generally similar in their mineral composition and facies organization are characterized by different thicknesses and numbers of constituting beds. Regional regularities in the development of sedimentary facies and, probably, variations in the influence of local sources of detrital material are observed along the structure strike. Hence, direct correlation of sediments at the rhythmostratigraphic level is impossible even for the neighboring pull-apart basins. In the case of the “plate” approach to correlation of riftogenic complexes, each additional borehole drilled along the strike of the shear system results in the appearance of new local stratigraphic units, which can at best correlate only in neighboring boreholes but do not correlate along the strike of the entire structure. The available correlation schemes of preplate sediments reflect precisely such a situation.

We understand that the proposed seismostratigraphic elements need further improvement, specification, and comprehensive verification. We hope that the defined seismocomplexes may be useful for the development of a detailed stratigraphic scheme for this complex and rather enigmatic region.

ACKNOWLEDGMENTS

We express our sincere gratitude to our Russian and Belarussian colleagues for planning, organizing, and conducting joint studies and constructive criticism. We are particularly grateful to V.I. Gorbachev, L.D. Tsvetkov, I.S. Gribova, O.A. Esipko (Nedra Federal State Unitary Enterprise, Yaroslavl); Yu.B. Konoval'tsev and A.I. Filin (Expedition no. 2, Spetsgeofizika Federal State Unitary Enterprise, Emmaus Settlement, Tver region); S.L. Kostyuchenko (VNIIGeofizika Federal State Unitary Enterprise, Moscow); A.M. Kovkhuto and Ya.G. Gribik (Department of Natural Resources and Environment Protection, Belarus Republic); and R.G. Garetsky, R.E. Aizberg, M.A. Nagornyi, and N.V. Veretennikov (Institute of Geology and Geophysics, National Academy of Sciences, Belarus Republic). We also thank Corresponding Member of the Russian Academy of Sciences A.V. Maslov for his valuable comments on the issues under consideration.

This work was accomplished under the thematic studies of the Laboratory of the Comparative Analysis of Sedimentary Basins (GIN RAN) and was supported by the Scientific School of Academician Yu.G. Leonov (project no. NSh-5508.2008.5).

REFERENCES

- Aizberg, R.E., Geodynamic Evolution of the Pripyat Paleorift Trough, *Dokl. Akad. Nauk BSSR*, 1986, vol. 30, no. 5, pp. 460–463.
- Aksenov, E.M., History of Geological Evolution of the East European Craton in the Late Proterozoic, *DSc (Geol.-Miner.) Dissertation*, St. Petersburg: Inst. Geol. Geokhim. Dokembriya Ross. Akad. Nauk, 1998.
- Anatol'eva, A.I., *Domezoiskie krasnotsvetnye formatsii* (Pre-Mesozoic Red-Colored Formations), Novosibirsk: Nauka, 1972.
- Batchelor, R.A. and Bowden, P., Petrogenetic Interpretation of Granitoid Rock Series Using Multicratonic Parameters, *Chem. Geol.*, 1985, vol. 48, pp. 43–55.
- Bogdanova, S.V., Segments of the East European Craton, Abstracts of Papers, *EUROPROBE Symposium in Jablonna 1991* Polish Acad. Sci., Eur. Sci. Foundation, 1993, A-20(255), pp. 33–38.
- Bogdanova, S.V., Gorbatshev, R., and Stephenson, R.A., EUROBRIDGE: Palaeoproterozoic Accretion of Fennoscandia and Sarmatia, *Tectonophysics*, 2001, vol. 339, pp. 34–49.
- Bogdanova, S.V., Bibikova, E.V., Postnikov, A.V., and Taran, L.N., Early Proterozoic Magmatic Belt of the Moscow Region, *Dokl. Akad. Nauk*, 2004, vol. 395, no. 3, pp. 376–380 [*Dokl. Earth Sci.* (Engl. Transl.), 2004, vol. 395, no. 3, pp. 315–318].
- Chamov, N.P., Structure and Formation Model of the Mid-Russian Aulacogen, in *Osadochnye basseiny: metodika izucheniya stroeniya i evolyutsii* (Sedimentary Basins: Methods for the Investigation of Structure and Evolution), Moscow: Nauchyi Mir, 2004, pp. 142–159.
- Chamov, N.P., Tectonic History and a New Evolution Model of the Mid-Russian Aulacogen, *Geotektonika*, 2005, vol. 39, no. 3, pp. 3–22 [*Geotectonics* (Engl. Transl.), 2005, vol. 39, no. 3, pp. 169–185].
- Chamov, N.P. and Gorbachev, V.I., Structure and Rock Composition of the Bel'sk Uplift of the near Moscow Aulacogen, *Byull. Mosk. O-va Ispyt. Priro., Otd. Geol.*, 2004, vol. 79, no. 4, pp. 3–10.
- Chamov, N.P. and Kostyleva, V.V., The Mid-Russian Aulacogen: Late Riphean System of Postcollision Tension in the Russian Plate, in *Geologiya, geokhimiya, geofizika na rubezhe XX i XXI vekov* (Geology, Geochemistry, and Geophysics at the Turn of XX and XXI Centuries), Moscow: SVYaZ-PRINT, 2002, vol. 1, pp. 114–115.
- Chamov, N. and Murdmaa, I., Coarse Fraction Minerals of Sands in Cascadia Margin Sediments, Leg 146 ODP, Abstracts of Papers, *Proc. Ocean Drill. Progr., Sci. Res.*, College Station, TX: ODP, 1995, vol. 146, no. 1, pp. 33–43.
- Chamov, N.P., Kostyleva, V.V., Veis, A.F., and Gorbachev, V.I., Late Riphean Sedimentation in the Central Russian Aulacogen, *Litol. Polezn. Iskop.*, 2003, vol. 38, no. 5, pp. 539–550 [*Lithol. Miner. Resour.* (Engl. Transl.), 2003, vol. 38, no. 5, pp. 458–467].
- Chamov, N.P., Kostyleva, V.V., Gorbachev, V.I., Gribova, I.S., Esipko, O.A., Konoval'tsev, Yu.B., and Filin, S.I., New Data on the Molokovo Basin Formation Mechanism (Russian Platform), *Geotektonika*, 2002, vol. 36, no. 3, pp. 9–21 [*Geotectonics* (Engl. Transl.), 2002, vol. 36, no. 3, pp. 176–187].

- Garetsky, R.G., Aulacogens in Platforms of Northern Eurasia, *Geotektonika*, 1995, vol. 30, no. 4, pp. 16–28.
- Garetsky, R.G., Sedimentary Basins of the Ancient Platform, *Vest. OGGGGN Ross. Akad. Nauk*, 1999, vol. 10, no. 4. URL: http://www.scgis.ru/russian/cp1251/h_dgggms/4-99/garetskiy.htm#begin.
- Garetsky, R.G., Karataev, G.I., Zlotsky, G., Astapenko, V.N., Belinsky, A.A., and Terletsky, V.V., Eurobridge Seismic Working Group, Seismic Velocity Structure across the Fennoscandia-Sarmatia Suture of the East European Craton beneath the EUROBRIDGE Profile through Lithuania and Belarus, *Tectonophysics*, 1999, vol. 314, pp. 193–217.
- Gee, D.G. and Stephenson, R.A., *The European Lithosphere: An Introduction European Lithosphere Dynamics*, Gee, D.G. and Stephenson, R.A., Eds., London: Geol. Soc. Mem., 2006, no. 32, pp. 1–9.
- Geisler, A.N., Experience of Geochronological Correlations and Paleogeography of the Late Proterozoic Deposits in the Northern and Central Parts of the Russian Platform, Abstracts of Papers, *Materialy po geol. evropeiskoi territorii SSSR* (Proc. Geology of the European Territory of the USSR), Leningrad: Nedra, 1966, pp. 32–57.
- Geologiya Belarusi* (Geology of Belarus) Makhnach, A.S., Garetsky, R.G., and Matveev, A.V., Eds., Minsk: Inst. Geol. Nauk Nats. Akad. Nauk Belarusi, 2001.
- Gordasnikov, V.N. and Troitskii, V.N., The Mid-Russian Aulacogen: The Main Structure of the Moscow Syncline, *Otech. Geol.*, 1966, no. 12, pp. 35–47.
- Kapustin, I.N., Vladimirova, T.I., Fedorov, D.L., et al., *Gipsometricheskaya karta poverkhnosti kristallicheskogo fundamenta tsentral'noi i severnoi chastei Vostochno-Evropeiskoi platformy mashtaba 1 : 2500000* (Hypsometric Map of the Crystalline Basement Surface in the Central and Northern Parts of the East European Craton, Scale 1 : 2500000), St. Petersburg: Vseross. Geol. Razved. Inst., 2001.
- Keller, B.M., Upper Proterozoic of the Russian Platform (Riphean and Vendian), in *Ocherki po regional'noi geologii SSSR* (Essays on Regional Geology of the USSR), Moscow: Nauka, 1968, no. 2.
- Kheraskova, T.N., Volozh, Yu.A., Andreeva, N.K., et al., New Data on Structure and Accumulation Conditions of Riphean-Early Vendian Sedimentation in the Central Russian Aulacogen System, *Geol. Vest. Tsent. Raionov Rossii*, 2001, no. 1, pp. 10–22.
- Kheraskova, T.N., Volozh, Yu.A., Vorontsov, A.K., et al., Sedimentation Conditions at the Central East European Platform in Riphean and Early Vendian, *Litol. Polezn. Iskop.*, 2002, vol. 37, no. 1, pp. 77–92 [*Lithol. Miner. Resour.* (Engl. Transl.), 2002, vol. 37, no. 1, pp. 68–81].
- Kirsanov, V.V., Issue of the Stratigraphy of Cambrian Rocks in the Axial Moscow Syncline, *Dokl. Akad. Nauk SSSR*, 1968, vol. 178, no. 5, pp. 1160–1163.
- Klevtsova, A.A., The Main Riphean Stages of Sedimentation in the Russian Platform (Early and Middle Stages), *Izv. Vyssh. Uchebn. Zaved., Geol. Razved.*, 1976, no. 7, pp. 3–15.
- Klevtsova, A.A., The Upper Proterozoic-Lower Paleozoic of the Moscow Syncline: Problems of Boundaries, *Geol. Geofiz. Razrabotka Neft. Mestorozhd.*, 2000, no. 12, pp. 33–42.
- Klevtsova, A.A., The Fourth Riphean Subdivision and Baikal Troughs in the East European Craton, *Izv. Vyssh. Uchebn. Zaved., Geol. Razved.*, 2003, no. 3, pp. 25–29.
- Kostyleva, V.V. and Simanovich, I.M., Mineralogy of Riphean Sandstones in the Orsha Depression: Significance for Stratigraphy and Tectonics, *Byull. Mosk. O-va Ispyt. Prir., Otd. Geol.*, 2007, vol. 82, no. 2, pp. 57–65.
- Kostyleva, V.V., Chamov, N.P., Simanovich, I.M., and Anikeeva, O.V., Evolutionary Stages of Riphean Sedimentary Basins in the Central East European Platform (with the Kresttsy and Pavlov Posad Sedimentary Basins as Example), *Litol. Polezn. Iskop.*, 2001, vol. 36, no. 4, pp. 408–417 [*Lithol. Miner. Resour.* (Engl. Transl.), 2001, vol. 36, no. 4, pp. 353–361].
- Kostyuchenko, S.L. and Ismail-Zade, A.T., Nature of Intense Sedimentation Phases in the Moscow Syncline Based on the Results of Deep Investigation and Quantitative Analysis of Borehole Sections, *Razved. Okhr. Nedr.*, 1998, no. 5, pp. 36–40.
- Kostyuchenko, S.L. and Solodilov, L.N., The Geological Structure of Muscovia: Deep Structure and Tectonics, *Byull. Mosk. O-va Ispyt. Prir., Otd. Geol.*, 1997, vol. 72, no. 5, pp. 6–17.
- Kostyuchenko, S.L., Egorkin, A.V., and Solodilov, L.N., Tectonic Model of Precambrian of the Moscow Syncline Based on the Results of Regional Investigations, *Razved. Okhr. Nedr.*, 1995, no. 5, pp. 8–12.
- Kostyuchenko, S.L., Egorkin, A.V., Solodilov, L.N., et al., Genetic Types of Precambrian Rifts in the Mezen-Lower Volga Divergent Belt of the East European Platform Based on the Results of Deep Investigations, *Razved. Okhr. Nedr.*, 1996, no. 4–5, pp. 46–53.
- Krogh, T., A Low Contamination Method for Hydrothermal Decomposition of Zircon and Extraction of U and Pb for Isotopic Age Determination, *Geochim. Cosmochim. Acta*, 1973, vol. 37, pp. 485–494.
- Kuz'menko, Yu.T. and Shik, S.M., A Refined Stratigraphic Scheme of Riphean Rocks in Central European Russia (Eastern Part of the Orsha Depression and Kresttsy and Soligalich Aulacogens), *Byull. Mosk. O-va Ispyt. Prir., Otd. Geol.*, 2006, vol. 81, no. 2, pp. 29–39.
- Ludwig, K.R., Pb Dat for MS-DOS, Version 1.21. U.S. Geol. Survey Open-File Rept. 88–542, 1991.
- Ludwig, K.R., *ISOPLOT/EX (Version 2.00). A Geochronological Toolkit for Microsoft Excel*, Berkeley Geochron Center, 1999, Spec. Publ. no. 1a.
- Makhnach, A.S., Veretennikov, N.V., Shkuratov, V.I., et al., Stratigraphy of Upper Proterozoic Rocks in Belarus, *Izv. Akad. Nauk SSSR, Ser. Geol.*, 1975, no. 3, pp. 90–102.
- Makhnach, A.S., Veretennikov, N.V., Shkuratov, V.I., and Bordon, V.E., *Rifei i vend Belorussii* (The Riphean and Vendian of Belarus), Minsk: Nauka Tekhnika, 1976.
- Nagornyi, M.A., *Tektonika Volyno-Srednerusskoi sistemy progibov* (Tectonics of the Volyn-Mid-Russian Depression System), Minsk: Nauka Tekhnika, 1990.
- Nagovitsin, K.E., Microfossils and Stratigraphy of the Upper Riphean in the Southwestern Siberian Craton, *PhD (Geol.-Miner.) Dissertation*, Novosibirsk: Inst. Geol. Geofiz. Sib. Otd. Akad. Nauk, 2001.
- Nikolaev, V.G., Tectonic Evolution of the Moscow Syncline in the Riphean, *Geotektonika*, 1999, vol. 33, no. 6, pp. 59–65 [*Geotectonics* (Engl. Transl.), 1999, vol. 33, no. 6, pp. 474–479].
- Osadochnye basseiny: metodika izucheniya, stroenie i evolutsiya* (Sedimentary Basins: Investigation Method, Struc-

- ture, and Evolution), Leonov, Yu.G. and Volozh, Yu.A., Eds., Moscow: Nauchnyi Mir, 2004.
- Ostrovskii, M.O., The Main Stages of Structure Formation in Central Regions of the East European Craton in the Precambrian and Paleozoic, *DSc (Geol.-Miner.) Dissertation*, Moscow: Mosk. Geol. Razved. Inst., 1974.
- Ostrovskii, M.I., Zolotov, A.N., Ivanova, T.D., and Sarkisov, Yu.M., The Riphean-Early Paleozoic Stage of Sedimentary Cover Formation in the Central and Northern Regions of the East European Craton, *Otech. Geol.*, 1975, no. 10, pp. 87–97.
- Pyatiletov, V.G., Late Precambrian Microfossils of the Uchur-Maya Region, in *Pozdnii dokembrii i rannii paleozoi Sibiri. Vend i rifei* (Late Precambrian and Late Paleozoic in Siberia: Vendian and Riphean), Novosibirsk: Izd. Inst. Geol. Geokhim. Sib. Otd. Akad. Nauk SSSR, 1988, pp. 47–94.
- Razlomy zemnoi kory Belarusi* (Faults in the Earth's Crust of Belarus), Aizberg, R.E., Ed., Minsk: Krasiko-Print, 2007.
- Reading, H.G., Collinson, J.D., Allen, P.A., et al., *Sedimentation Environments*, New York: Elsevier, 1978. Translated under the title *Obstanovki osadkonakopleniya i fatsii*, Moscow: Mir, 1990, vol. 1.
- Scheidegger, R.F., Kulm, L.D., and Piper, D.J.W., Heavy Mineralogy of Unconsolidated Sands in Northeastern Pacific Sediments: Leg 18 DSDP, Abstracts of Papers, *Proc. Deep Sea Drill. Proj., Init. Rep.* Washington: U.S. Govt. Print. Office, 1973, vol. 18, pp. 877–887.
- Shatskii, N.S., Depressions of the Donetsk Type, in *Izbrannye trudy* (Selected Works), Moscow: Nauka, 1964, vol. II, pp. 544–553.
- Shutov, V.D., *Mineral'nye paragenезы grauвакковых комплексов* (Mineral Assemblages of the Graywacke Complexes), Moscow: Nauka, 1975.
- Simanovich, I.M., *Kvarts peschanykh porod* (Quartz of Sedimentary Rocks), Moscow: Nauka, 1974.
- Simanovich, I.M., Mineralogy and Petrography of Riphean Rocks in the Moscow Graben, *Litol. Polezn. Iskop.*, 2000, vol. 35, no. 5, pp. 25–37 [*Lithol. Miner. Resour.* (Engl. Transl.), 2000, vol. 35, no. 5, pp. 475–483].
- Sklyarov, E.V., Mazukabzov, A.M., and Mel'nikov, A.I., *Kompleksy metamorficheskikh yader kordil'erskogo tipa* (Metamorphic Core Complexes of the Cordilleras Type), Novosibirsk: Izd. Sib. Otd. Ross. Akad. Nauk, Nauchno-Issled. Tsentr Ob"ed. Inst. Geol. Geokhim. Mineral., 1997.
- Stacey, J.S. and Kramers, J.D., Approximation of Terrestrial Lead Isotope Evolution by a Two-Stage Model, *Earth Planet. Sci. Lett.*, 1975, vol. 26, no. 2, pp. 207–221.
- Valeev, R.I., Klubov, V.N., and Ostrovskii, M.I., Comparative Analysis of the Formation Conditions and Spatial Distribution of Aulacogens in the Russian Platform, *Otech. Geol.*, 1969, no. 4, pp. 58–67.
- Valeev, R.N., *Avlakogeny Vostochno-Evropеiskoi platformy* (Aulacogens in the East European Craton), Moscow: Nedra, 1978.
- Veis, A.F., Riphean and Vendian Microfossils in the Uchur-Maya and Turukhansk Regions of Siberia, *Izv. Akad. Nauk SSSR, Ser. Geol.*, 1988, no. 5, pp. 47–64.
- Veis, A.F. and Vorob'eva, N.G., Microfossils of the Siberian Hypostratotype of Riphean (Omakhta, Kandyk, and Ust-Kirba Microbiotas), *Stratigr. Geol. Korrelyatsiya*, 2002, vol. 10, no. 1, pp. 27–54.
- Veretennikov, N.V., Makhnach, A.S., Laptsevich, A.G., and Shkuratov, V.I., Stratigraphic Scheme of Riphean Rocks in Belarus, *Litosfera*, 2005, vol. 22, no. 1, pp. 27–35.
- Vladimirova, T.I., Kapustin, I.N., Orlov, V.I., and Fedorov, D.L., *Ob"yasnitel'naya zapiska k gipsometricheskoi karte poverkhnosti kristallicheskogo fundamenta tsentral'noi i severnoi chasti Vostochno-Evropеiskoi platformy masshtaba 1 : 2 500 000* (Explanatory Note to the Hypsometric Map of the Crystalline Basement Surface in the Central and Northern Parts of the East European Craton, Scale 1 : 2 500 000), St. Petersburg: Vseross. Geol. Razved. Inst., 2001.
- Zen, E. and Hammarstrom, J.M., Magmatic Epidote and Its Petrologic Significance, *Geology*, 1984, vol. 12, pp. 515–518.